CrossMark

ORIGINAL ARTICLE

Degradation of groundwater quality in coastal aquifer of Sabratah area, NW Libya

Nawal Alfarrah[1,2] · Gebremedhin Berhane[1,3] · Charles Bakundukize[4] ·
Kristine Walraevens[1]

Abstract Overextraction of groundwater is widely occurring along the coast where good quality groundwater is at risk, due to urbanization, tourist development and intensive agriculture. The Sabratah area at the northern central part of Jifarah Plain, Northwest Libya, is a typical area where the contamination of the aquifer in the form of saltwater intrusion, gypsum/anhydrite dissolution and high nitrate concentrations is very developed. Fifty groundwater samples were collected from the study area and analysed for certain parameters that indicate salinization and pollution of the aquifer. The results demonstrate high values of the parameters electrical conductivity, sodium, potassium, magnesium, chloride and sulphate which can be attributed to seawater intrusion. The intensive extraction of groundwater from the aquifer reduces freshwater outflow to the sea, creates drawdown cones and lowering of the water table to as much as 30 m below mean sea level. Irrigation with nitrogen fertilizers and domestic sewage and movement of contaminants in areas of high hydraulic gradients within the drawdown cones probably are responsible for the high nitrate concentration towards the south of the region. Seawater intrusion and deep salt water upconing result in general high SO_4^{2-} concentrations in groundwater near the shoreline, where localized SO_4^{2-} anomalies are also due to the dissolution of sebkha deposits for few wells in the nearby sebkhas. Upstream, the increase in SO_4^{2-} concentrations in the south is ascribed to the dissolution of gypsum at depth in the upper aquifer.

Keywords Saltwater intrusion · Excessive pumping · Groundwater pollution · Gypsum dissolution · Sabratah

Introduction

Water is essential for peoples' health and socioeconomic development. With the improvement in living standards, people have not only put efforts into safeguarding sufficient quantities of water resources, but have also paid more attention to increasing water quality (Wu et al. 2013; Wang et al. 2014). The ever-growing demand for freshwater for a number of human purposes has become a worldwide cause of concern. Nowadays, groundwater reserves are exposed to intensive exploitation, mainly from strong agricultural development accompanied by low recharge infiltration to the phreatic aquifers (Walraevens et al. 1994; Van Camp and Walraevens 2009; Van Camp et al. 2010, 2012, 2013; Mjemah et al. 2011; Radfar et al. 2013; Werner et al. 2012), that may lead to serious problems in coastal zones where freshwater reservoirs are connected to the sea (Masciopinto 2006; Mjemah et al. 2009; Van Camp et al. 2014), resulting in deterioration in groundwater quality. The agricultural development also leads to changes in land cover and land use, with declining natural vegetation (Kassa et al. 2015; Grimaldi et al. 2015; Walraevens et al. 2015; Wildemeersch et al. 2015; Wang et al. 2016).

✉ Nawal Alfarrah
Nawalr2003@yahoo.com

Kristine Walraevens
Kristine.Walraevens@ugent.be

1 Laboratory for Applied Geology and Hydrogeology, Department of Geology, Ghent University, Krijgslaan 281 S8, 9000 Ghent, Belgium

2 Geology Department, Az Zawiyah University, Az Zawiyah, Libya

3 Geology Department, Mekelle University, Mekelle, Ethiopia

4 Geology Department, Burundi University, Bujumbura, Burundi

This situation is particularly observed in coastal areas of the Mediterranean region of North Africa and the Middle East, where surface waters are limited and population densities are large. Overexploitation of groundwater in these regions is the major cause of seawater intrusion problems (Ben-Asher et al. 2000; Edmunds and Milne 2001; Gordu et al. 2001; Yazicigil and Ekmekci 2003; Karahanoglu and Doyuran 2003; Demirel 2004; Camur and Yazicigil 2005; De Montety et al. 2008; Custodio 2010; Alfarrah et al. 2011). Groundwater quality patterns are complex because of the input from many different water sources (Trabelsi et al. 2007; Zouhri et al. 2008). These include seawater intrusion, ascending deep saline groundwater and anthropogenic sources such as wastewater or irrigation return flow (Coetsiers and Walraevens 2009; Walraevens et al. 2013).

Salinization is represented by the increase in total dissolved solids (TDS) and some specific chemical constituents including, Na^+, Mg^{2+} and SO_4^{2-}; Walraevens et al. 1993a, b; Morell et al. 1996; Sukhija et al. 1996; Chaouni Alia et al. 1997; GiméNez and Morell 1997; Walraevens et al. 2007; Mtoni et al. 2012, 2013; Da'as and Walraevens 2013). The main sources of SO_4^{2-} in groundwater next to mixing with sea water are oxidation of pyrite (FeS_2), and the dissolution of gypsum and anhydrite (Coetsiers and Walraevens 2006; Coetsiers et al. 2009).

In Libya, numerous irrigation regions are located near the coast, principally in the northern part of Jifarah Plain, including Sabratah region, where extensive irrigated areas have been established in the late 1970s and have evolved into advanced agricultural production zones; these activities are primarily dependent on groundwater extraction. Sabratah is the area of the highest agricultural activity of Jifarah Plain and is one of the most important touristic centres. The archaeological site in Sabratah was registered as a UNESCO World Heritage Site in 1982 and has substantially contributed to touristic expansion. Water overextraction for urbanization and tourism is concentrated in the coastal part of Sabratah, which has strongly developed since the beginning of the 1980s.

This situation has led to two significant problems linked to human activity: (1) salinization due to the formation of large piezometric drawdown cones, which have induced seawater intrusion by reversing the hydraulic gradients into aquifers, (2) direct input of nitrate mainly from fertilizers and sewage. Agriculture is based on intensive irrigation and fertilization to improve the soils. High pumping rates lead to aquifer drought, large water level drawdown and most of groundwater in the south being pumped from the lower part of the aquifer formation, which is comprising gypsum/anhydrite deposits.

The principal aquifer used by the population in Sabratah is the Upper Miocene–Pliocene–Quaternary aquifer system, known as "first aquifer" or "upper aquifer"; the aquifer is divided into a number of aquifer layers by less permeable intercalations; all layers are considered as one unconfined aquifer unit (Alfarrah et al. 2013). The Sabratah upper aquifer is influenced by different sources of contamination, most serious is saltwater invasion (Alfarrah 2011). Sabratah area is a typical example showing the problems of coastal zones under high anthropogenic pressure in dryland regions. The objective of this paper was to investigate the hydrochemical processes that have caused salinization of groundwater in the main aquifer of Sabratah and to recognize the different sources of pollution, and their relation to the intense water withdrawal.

Materials and methods

Sabratah (also spelled Subrata) lies on the Mediterranean coast about 66 km west of Tripoli (Fig. 1). The region of study is located in the western part of central Jifarah Plain between 32°49′31″ North and 12°37′5″ East. This area extends for about 20 km along Sabratah–Surman coastal area and about 22 km inland. Topography is rising towards the south, a general trend in overall Jifarah Plain, which is bounded to the south by Jabal Nafusa Mountains.

The shortage of good quality water from surface sources has made groundwater to be very important in the study area. The scarcity of water in Sabratah is becoming more pronounced due to the increase in the population coupled with improvement in the standard of living over the last few decades. The area of the study accommodates dense population with more than 93,000 inhabitants mostly concentrated in the coast.

The climate in the study area is arid to semi-arid and typically Mediterranean, with irregular annual rainfall. The average annual rainfall and evapotranspiration rates are 250 and 1535 mm/year, respectively (Alfarrah 2011). The estimation of groundwater exploitation (in the whole Jifarah Plain) from the main upper aquifer shows that the total amount of groundwater pumped in the Jifarah Plain for domestic, industrial and agricultural uses amounts to 1201.30 Mm^3/year (Alfarrah 2011). For drinking water supply and domestic wells, the overall amount pumped is 6% of the total amount of groundwater extraction. The yield of irrigation wells was estimated to be 1123 Mm^3/year, which is equal to 93% of the total amount of groundwater extraction. The industrial sector pumps only 1% of the total groundwater exploitation in the plain.

Geological and hydrogeological setting

The Sabratah Basin is situated on the continental margin of Africa. Although the basin is thought to be underlain by
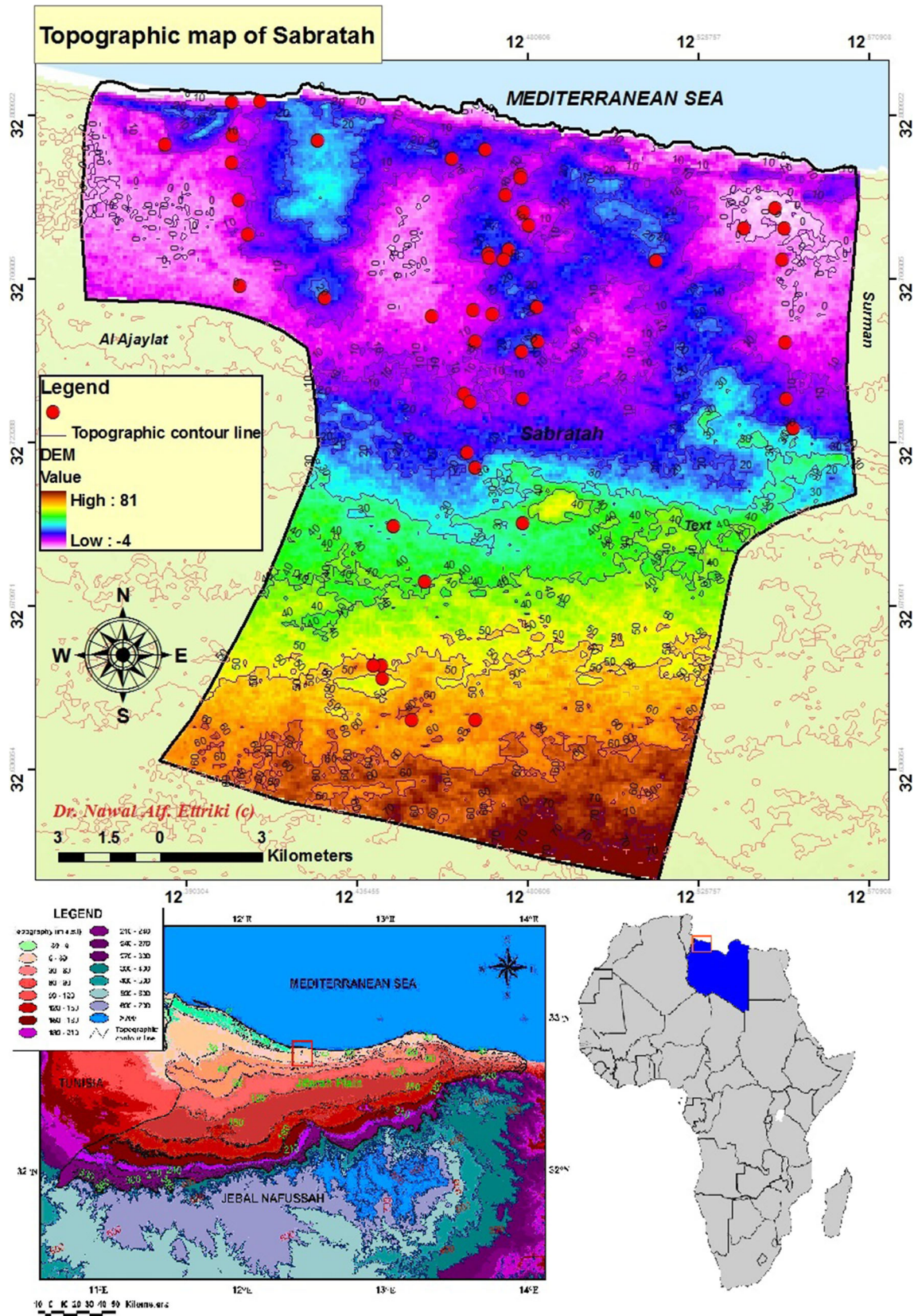
Fig. 1 Location and topography of the study area in Jifarah Plain in Libya

Palaeozoic rocks, the oldest encountered in boreholes are Triassic in age. These are continental, passing upwards into evaporites, a sequence thought to represent the progressive subsidence of the margin during major Mesozoic extension of the Tethyan Ocean. Continued subsidence through the Jurassic and Early Cretaceous led to the deposition of marine sequences.

Figure 2 represents the geological map for Sabratah region with the sampling boreholes location. The sediments of the Sabratah region have been deposited in early Mesozoic times in a near shore lagoonal environment. The lithology of the upper aquifer varies widely and includes detrital limestone, dolomite, gravel, marl, clay, silt, sand, sandstone, gypsum/anhydrite and calcarenite. To the south of Sabratah, the lower layer of the main aquifer is composed of gypsiferous limestone, anhydrite and sandstone, producing highly mineralized sulphate water in this area (Alfarrah 2011). Middle Miocene clay separates the upper
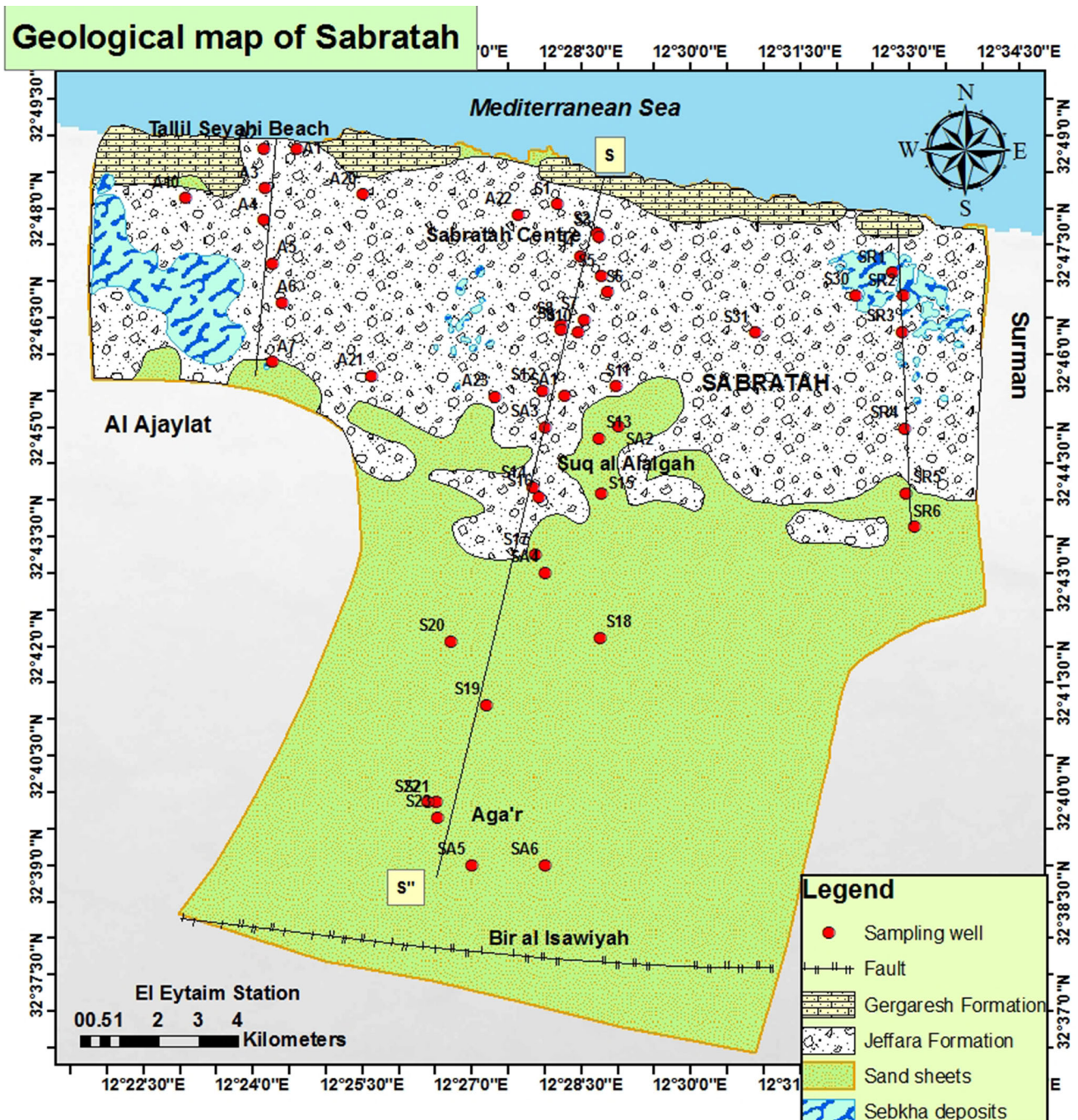

Fig. 2 Geological map of Sabratah with location of sampled wells and of hydrochemical cross section

aquifer system in the area from the middle aquifer. The bottom of the main aquifer varies between 30 m in the north and 200 m to the south of the region, where depths of the pumping wells are between 30 and 180 m. Most of these wells have productivity of about 50–80 m³/h (Al-farrah et al. 2013).

The geological deposits, relevant to the hydrogeology of the area, comprising the upper aquifer formations, are given in Table 1.

It follows that coastal dunes are composed of aeolian materials containing a high amount of gypsum. In some locations, they are composed of pure gypsum (98%) mainly in the immediate vicinity of the sebkhas (Libyan Industrial Research Centre 1995).

Methodology

Sampling and analysis

Water samples were collected from 50 wells (mostly 20–180 m deep during the dry period from September to November of 2008. The samples were collected during pumping, and the depth to the water level was measured in static conditions with water level meter, using ground surface as a reference.

Samples were collected along three vertical profiles perpendicular to the coast (Fig. 2), up to 20 km inland. All water samples were filtered through 0.45 μm MF-Millipore membrane filters in the field and then stored in polyethylene bottles. Two samples were collected from each sampling site, one for anions determination, the other for cations analysis; the latter sample was acidified with nitric acid to prevent metal precipitation.

Physical properties were measured including: water level, temperature, pH and electrical conductivity. Flame atomic absorption spectrometry (Varian) was used to analyse cations (Na^+, K^+, Mn^{2+}, Fe^{Total}, Ca^{2+}, Mg^{2+}, Zn^{2+}, Si^{4+}) and molecular absorption spectrophotometry (Shimadzu) was used to analyse anions (Cl^-, NO_3^-, NO_2^-, SO_4^{2-}, PO_4^{3-}) and NH_4^+ ion selective electrode was used to measure F^-. The titration method was used for the determination of carbonate (CO_3^{2-}) and bicarbonate (HCO_3^-) using dilute HCl acid with end points at pH 8.2 and 4.3, respectively. Standard Methods for Examination of Water and Wastewater (American Public Health Association 1985) were used, and analyses were performed at the Laboratory for Applied Geology and Hydrogeology at Ghent University.

Ionic balance was computed for each sample to assess the accuracy of analyses. All samples exhibited imbalances of less than 5%.

Hydrochemical methods

The hydrochemical evolution is investigated based on the calculation of the saturation indices (SI), the ion deviations (Δm_i) from conservative mixture of freshwater/sea water, graphical presentation including Piper diagram, ionic ratios calculation, elaboration of hydrochemical profiles and water quality parameter mapping.

PHREEQC is the international standard reference program for hydrochemical modelling, developed by the United State Geological Survey (USGS). The program can be used for speciation, batch-reaction, one-dimensional transport, and inverse geochemical calculations. Using the PHREEQC 2.16 program (Parkhurst and Appelo 1999), saturation indices were calculated for calcite, dolomite, halite and gypsum.

The potential deviations from the simply mixed composition of different end members results from various chemical processes are known as the ionic deltas. When is positive, groundwater is getting enriched for ion i whereas a negative value indicates a depletion of the ion i compared to the theoretical mixing (Andersen et al. 2005).

The ionic deltas quantify the extent of chemical reactions that affect groundwater composition, additional to mixing.

The seawater fraction (f_{sea}) in the groundwater was estimated using chloride concentration (Custodio and Bruggeman 1987). The seawater fraction of a conservative mixing is calculated as follows (Appelo and Postma 2005):

$$f_{sea} = \frac{m_{Cl^-,sample} - m_{Cl^-,fresh}}{m_{Cl^-,sea} - m_{Cl^-,fresh}} \quad (1)$$

where $m_{Cl^-,sample}$ is the concentration of Cl^- in the sample expressed in mmol/l, $m_{Cl^-,fresh}$ is the concentration of Cl^- in the freshwater expressed in mmol/l, $m_{Cl^-,sea}$ is Cl^- concentration in the seawater end member in mmol/l (for Mediterranean sea water, $m_{Cl^-,sea} = 645$ mmol/l (value taken from the literature; Da'as and Walraevens 2010). The seawater fraction is used for determining the concentration of each ion i resulting from the conservative mixing of sea water and the freshwater (Appelo and Postma 1993):

$$m_{i,mix} = f_{sea} \cdot m_{i,sea} + (a - f_{sea}) \cdot m_{i,fresh} \quad (2)$$

where m_i is concentration of an ion i in mmol/l and subscripts mix, sea and fresh are indicating the conservative mixture and end members (sea water and freshwater). The difference between the concentration of the conservative mixture $m_{i,mix}$ (mmol/l) and the measured one $m_{i,sample}$ (mmol/l) represents the concentration resulting from any chemical reaction occurring with mixing:

$$\Delta m_i = m_{i,reaction} = m_{i,sample} - m_{i,mix} \quad (3)$$

Table 1 Summary of the stratigraphic section of the upper aquifer formations in the coastal area of Jifarah Plain

Period	Epoch	Hydrogeology	Formation	Typical lithology	Thickness (m)
Quaternary	Holocene	Upper Miocene–Pliocene–Quaternary aquifer	Wadi deposits	Loose gravel, loam	5–150
			Sand beach	Shell and silica sand	
			Sand dunes and sand sheets	Shell fragments, silica sands and gypsum	
			Sebkha deposits	Gypsum	
			Fluvial–Eolian deposits	Silt, clay, marl and fine sand	
			Gergaresh formation	Conglomerate, sandstone, silt, sandy limestone	
	Pleistocene		Jeffara formation	Silt, sand and gravel caliche bands	
			Qsar al Haj formation	Alluvial fans and cones	
			Al Kums formation	Limestone, dolomite	
	Pliocene–quaternary		Al Assah formation	Silt, sand, gravel, limestone, gypsum	25–250
Tertiary	Miocene				
	Middle		Middle Miocene clay		

End members of Mediterranean sea water and freshwater from the upper aquifer are used in the calculation. For Mediterranean sea water where $Cl^- = 645$ mmol/l, the seawater fraction has been calculated as:

$$f_{sea} = \frac{m_{Cl^-, sample}}{645} \qquad (4)$$

Stuyfzand classification is very appropriate for areas subjected to seawater intrusion.

This hydrochemical classification system combines excellent features of existing classifications with new, strongly diagnostic criteria for subdivision. This results in an easier identification of cation exchange phenomena, e.g. due to salt or freshwater intrusion, and in the applicability to a broader spectrum of hydrochemical environments. A hierarchical structure, high flexibility and logical coding guarantee an easy handling of a sophisticated system (Stuyfzand 1986).

The determination of a water type implies the successive determination of the main type (based on chloride concentration), the type (based on total hardness), the subtype (based on dominant cation and anion) and finally the class of the water sample. Each of the four levels of subdivision contributes to the total code (and name) of the water type (Stuyfzand 1986, 1993; Mollema et al. 2013).

The *class* is highly useful to recognize freshening/salinization phenomena, as it provides information on cation exchange. For its determination, the sum of Na^+, K^+ and Mg^{2+} in meq/l, corrected for a sea salt contribution, is calculated (Eq. 5). The result indicates whether cation exchange has taken place, by assuming that Cl^- behaves conservatively.

$$\{Na^+ + K^+ + Mg^{2+}\} corrected$$
$$= [Na^+ + K^+ + Mg^{2+}] measured - 1.061 Cl^- \qquad (5)$$

where $-$ = indicates a saltwater intrusion, $+$ = indicates a freshwater encroachment and 0 = indicates an equilibrium.

For example, B4-NaCl$^-$ reads as: "brackish extremely hard sodium chloride water, with a $\{Na^+ + K^+ + Mg^{2+}\}$ deficit". This deficit often occurs during seawater invasion due to cation exchange reaction. According to Appelo and Postma (1993), the hydrogeochemical composition of coastal groundwater affected by seawater intrusion is mainly controlled by cation exchange next to the simple mixing process. These reactions are explaining the deviations of the concentrations of cations from conservative mixing of both waters.

Results and discussion

Water level and hydrodynamics

Figure 3 shows a piezometric map of Sabratah, and Fig. 4 is a hydrogeological profile constructed from the sea to the inland. The overall direction of groundwater flow in Jifarah Plain in general, including Sabratah, is from the south from Jabal Nafusa Mountains to the coast. The important storage withdrawal by overexploitation from the upper aquifer in Sabratah is causing continuous drawdown of the water level, seawater intrusion and the progressive groundwater quality degradation. Groundwater level is mostly low especially near to the coast, where zero and negative heads are recorded for the majority of wells. The piezometric level in depression cones in the central zone has dropped from 25 to 33 m below sea level (Fig. 3).

Sabratah profile is about 20 km long perpendicular to the sea (Fig. 4), starting from the sea and the city centre of Sabratah in the north to Bir al Isawiyah (Aga'r) in the south. Fifty wells were visited in the region. Their total depth is shallow (between 15 and 50 m) close to the coast and reaches 120 m southward. They are pumping for irrigation in the private farms and for domestic use.

Sabratah area is a very important case study in the arid and semi-arid region, where large stresses have been applied to the aquifer due to growing population and the important location of the area, its contribution to the agricultural output in Libya and its importance as a touristic city in the country. In this area, the largest depression cone along the coast of Jifarah Plain was formed as a result of overexploitation.

Sabratah belongs to the area with the highest agricultural activity in Jifarah Plain, especially in Suq al Alalqah at about 6 km from the coast and areas towards the south of the region. Large number of wells in the profile show negative heads with a minimum of $- 33$ m.a.s.l at the centre of depression cone. From Figs. 3 and 4, it can be concluded that, although the general groundwater flow is from south to north following the topography (see Fig. 1), locally in many cases flow is towards the reduced heads in the stressed areas.

Hydrochemical parameters

Major ions were analysed and pH, Eh, electrical conductivity (EC) and temperature were measured on all samples using WTW instrument. The temperature ranges between 19 and 25 °C, pH range is 6.71–8.21, Eh range is 128–463 mV, EC range is 805–15,650 μS/cm (25 °C), TDS range is 564–11,141 mg/l and chloride concentration ranges between 95 and 5282 mg/l. Table 2 shows analytical results of groundwater for some representative samples in Sabratah area.

Saltwater contains roughly 35,000 mg/l of dissolved solids, of which 19,000 mg/l is chloride (Lyles 2000). Consequently, the main cause of high chloride in coastal aquifers is most likely attributed to seawater intrusion.

EC is positively correlated with the concentration of ions, mainly Cl^- concentration. Figure 5 shows three zones
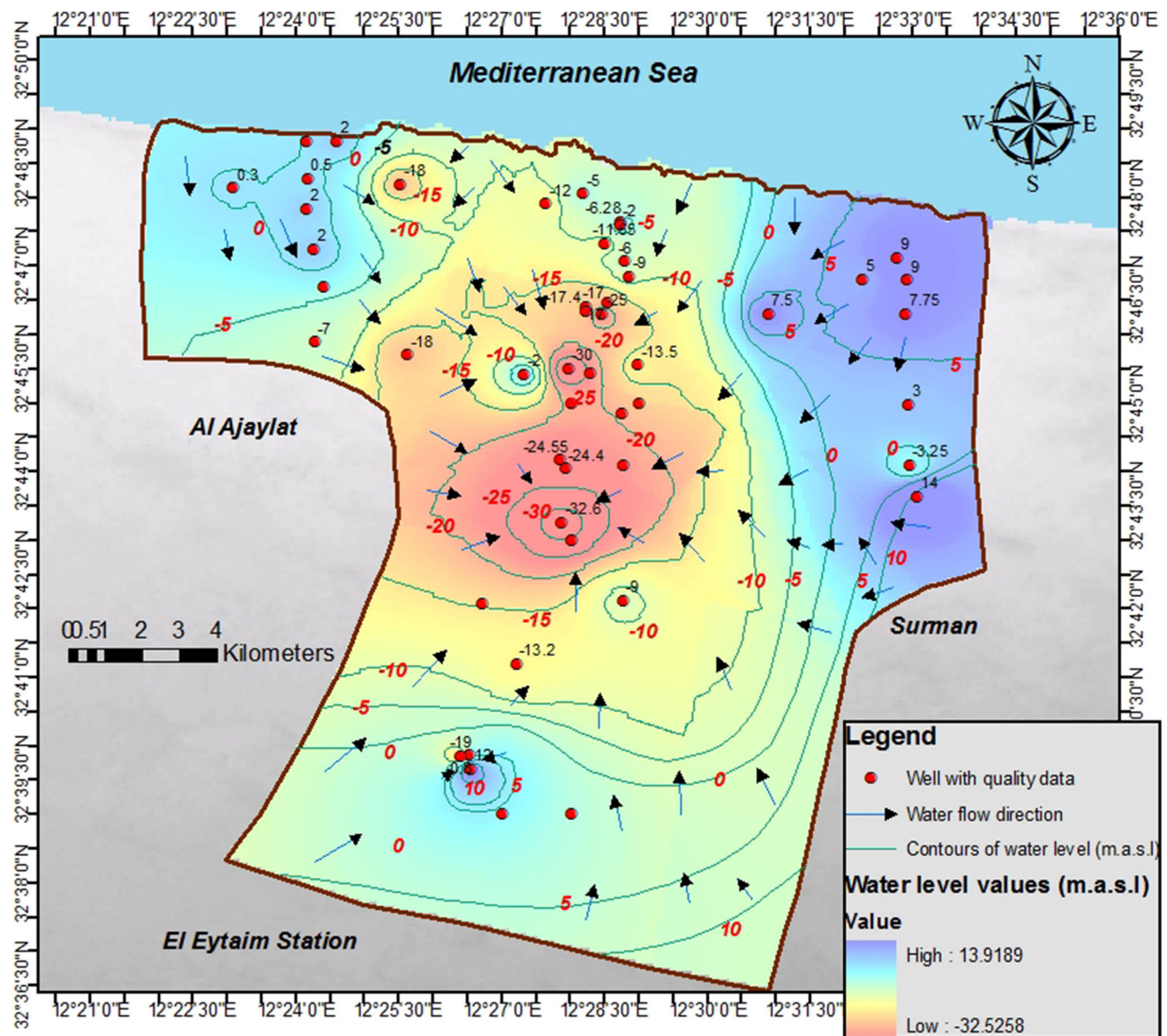
Fig. 3 Sabratah piezometric map with flow vectors

on a plot of Cl$^-$ versus EC: freshwater zone, mixing zone and intrusion. It shows that groundwater samples with Cl$^-$ exceeding 200 mg/l and EC exceeding $\sim$ 1000 μS/cm are most likely influenced by seawater intrusion. Groundwater samples that are characterized by EC between 1000 and 5000 μS/cm represent a mixing between freshwater and saltwater.

Figure 6 shows EC map for the analysed samples, and Fig. 7 is a map with the concentrations of Cl$^-$.

The high Cl$^-$ anomaly is mainly from mixing with sea water. These high concentrations of chloride are observed in most wells within some kilometres from the sea and are related to active seawater intrusion. But high Cl$^-$ is also found far inland at and nearby the depression cones. The concentration of Cl$^-$ decreases gradually towards the

south. High concentration of Cl$^-$ still can be found in many farther inland wells. The higher concentration of Cl$^-$ than the 250 mg/l value for standard drinking water at the south of the region can be linked to the synsedimentary marine influence of the groundwater, whereby deeper saline groundwater is affected by upconing due to groundwater exploitation.

The high concentration of major ions such as Cl, Na, Ca, K, Mg and a high EC indicate the presence of sea water in an aquifer (Mollema et al. 2015; Mollema 2016).

Sulphate concentration in Sabratah ranges from 29 to 2238 mg/l. Figure 8 shows spatial distribution of SO$_4^{2-}$ concentration in the study area. The main source for rising SO$_4^{2-}$ is mixing with sea water, which can add significant amounts of sulphate to freshwaters. High SO$_4^{2-}$ is mostly
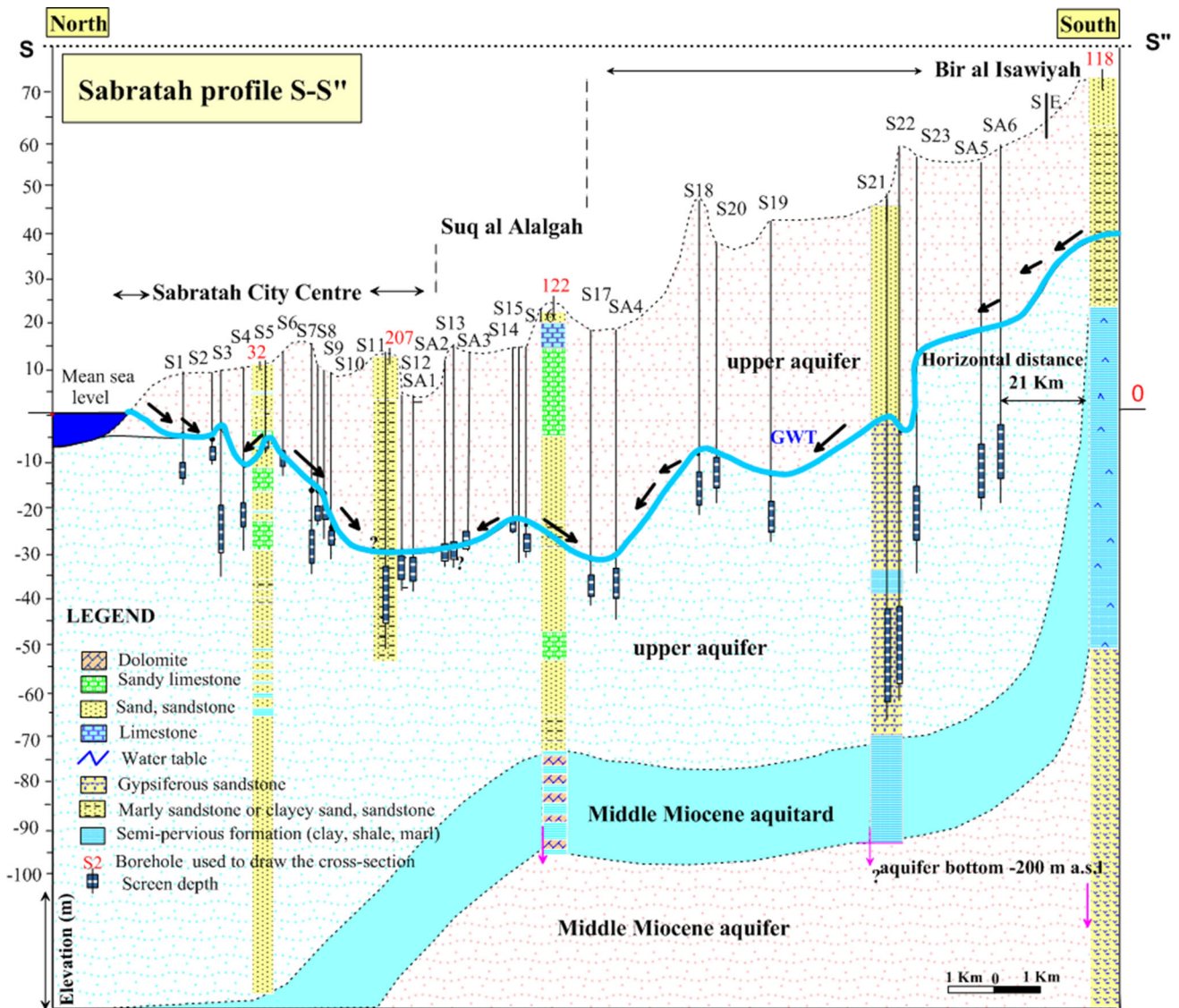
Fig. 4 Hydrogeological profile S–S″ in Sabratah. Cross section is indicated in Fig. 2

due to the high Cl⁻ concentration in the first aquifer, both in the seawater intrusion zones and in the depression cones, where deep saline water upconing occurs.

Towards the south of Sabratah region, a concentration higher than 1000 mg/l SO_4^{2-} is recorded, about 11 km from the sea to about 20 km inland, with much higher SO_4^{2-}/Cl⁻ compared to sea water. The main source of SO_4^{2-} in this zone is the dissolution of gypsum/anhydrite from the lower part of the aquifer, where gypsiferous sandstone, gypsiferous limestone and anhydrite are present. In this zone Cl⁻ concentration is low, excluding seawater intrusion as the source.

In the coastal area, high concentrations of SO_4^{2-} over 500 mg/l are observed at several wells (e.g. A4, A5, A23 and SR3). The additional source of high SO_4^{2-} for these wells is the dissolution of gypsum from the superficial sebkha deposits.

The high SO_4^{2-} in southern Sabratah is accompanied by high NO_3^- concentrations. Figure 9 shows the spatial distribution of NO_3^- in the study area. The average nitrate concentration of groundwater in the aquifer is about 63 mg/l, but contents as high as about 160 mg/l occur upstream in the south of the region. The high NO_3^- concentrations in these waters are a result of intensive agricultural activities mainly in the south of the region (> 100 mg/l is recorded for many wells), where high application of fertilizers is common during the last two decades (Alfarrah et al. 2011).

Irrigation with nitrogen fertilizers and domestic sewage and movement of contaminants in areas of high hydraulic gradients within the drawdown cones probably are responsible for localized peaks of the nitrate concentration at the central zone of the region.

Table 2 Selected results for physico-chemical parameters for groundwater samples in Sabratah area

| ID	Ca²⁺ (mg/l)	Mg²⁺ (mg/l)	Na⁺ (mg/l)	K⁺ (mg/l)	Fe²⁺/³⁺ (mg/l)	Mn²⁺ (mg/l)	NO₃⁻ (mg/l)	HCO₃⁻ (mg/l)	NO₂⁻ (mg/l)	CO₃²⁻ (mg/l)	Cl⁻ (mg/l)	SO₄²⁻ (mg/l)	pH	EC (µS/cm 25 °C)	T (°C)	Water level (m a.s.l)
A10	98.00	64.80	770.50	31.30	0.00	0.00	16.30	244.10	0.00	0.00	1091.90	451.50	7.30	4320	20	0.30
A4	652.20	252.10	1667.50	50.80	0.00	0.00	21.20	256.30	0.00	12.00	3949.10	547.50	7.65	11,960	25	2.00
A5	716.20	369.70	2748.50	74.30	0.00	0.00	19.90	360.00	0.00	24.00	5282.00	1546.60	7.88	15,650	24	2.00
A23	796.20	409.40	1840.00	50.80	0.00	0.00	12.30	897.00	0.00	0.00	3545.00	2012.50	6.71	11,970	23	− 2.00
S1	236.10	96.00	908.50	23.50	0.00	0.01	20.50	177.00	0.12	0.00	1474.70	677.20	7.87	5740	25	− 5.00
S2	120.30	38.80	568.00	11.00	0.02	0.00	49.69	395.89	0.00	0.00	651.58	422.10	7.60	3890	19	− 6.28
S3	184.00	135.70	989.00	19.50	0.00	0.00	9.60	238.00	0.00	0.08	1644.90	586.00	7.91	6120	24	− 2.00
S7	113.40	34.00	136.50	7.00	0.12	0.00	39.95	181.78	0.24	0.08	361.14	106.89	7.82	1500	20	− 17.00
S8	85.90	24.00	109.30	7.00	0.17	0.00	45.92	174.46	0.12	0.08	194.46	96.46	7.63	1186	22	− 17.00
S9	96.60	29.00	119.60	7.00	0.18	0.00	46.41	167.14	0.13	0.08	270.35	95.66	7.20	1412	23	− 17.40
S10	112.00	50.40	133.40	11.70	0.00	0.00	13.80	152.50	0.00	0.00	315.50	177.70	7.90	1528	24	− 25.00
S11	122.00	43.20	151.80	19.50	0.00	0.00	15.40	152.50	0.00	0.00	329.70	187.30	7.60	1627	24	− 13.50
S19	339.40	125.00	218.60	8.00	0.18	0.09	98.29	195.81	0.11	0.07	318.84	1166.62	7.30	3250	21	− 13.20
S22	782.00	228.00	389.00	11.00	0.27	0.26	77.47	183.00	0.13	0.08	863.60	2238.40	7.56	5380	21	− 19.00
S23	401.30	128.00	206.90	8.00	0.06	0.00	136.22	179.95	0.11	0.09	223.48	1242.42	7.38	3430	21	12.00
SR2	514.10	195.70	621.00	23.50	0.00	0.00	18.80	177.00	0.00	0.00	2052.50	384.00	7.04	6700	23	9
SR3	352.10	170.50	683.10	27.40	0.00	0.00	16.20	256.30	0.00	0.00	1244.30	1061.50	7.26	5500	24	7.75
SR4	224.10	80.40	188.60	11.70	0.00	0.00	23.20	189.20	0.00	0.00	560.10	331.40	7.89	2610	25	3.00
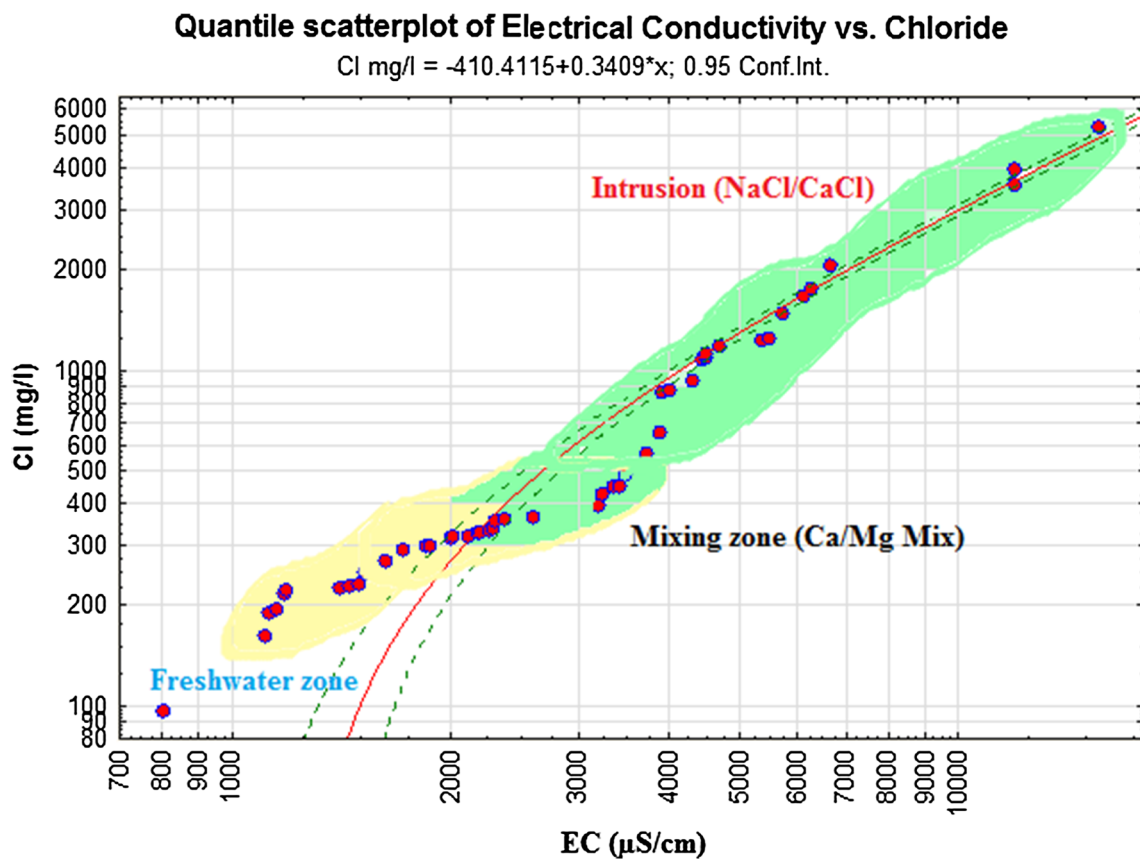
Fig. 5 A plot of chloride versus electrical conductivity showing fresh groundwater conditions, saltwater intrusion and mixing between the two end members

Out of 50 samples analysed, 58% have NO_3^- more than the highest desirable level of 45 mg/l (WHO 2008). For sulphate 78% have SO_4^{2-} higher than the highest desirable level of 200 mg/l and 32% have SO_4^{2-} more than the maximum permissible value of 500 mg/l according to WHO (2008); a maximum of 2238 mg/l was recorded southwards. Out of 50 analysed samples, 80% exceed the recommended Cl^- value for standard drinking water (250 mg/l) and 28% have Cl^- greater than the highest admissible level of 600 mg/l (WHO 2008).

Because of gypsum dissolution in groundwater, Ca^{2+} concentration in groundwater increases in several wells to significant levels (e.g. A23 with Ca^{2+} of 796 mg/l). Additionally, the dissolution of sebkha deposits contributes to the high concentration of Ca^{2+} in several nearby wells.

A comparison of certain parameters (Na^+, Ca^{2+}, Mg^{2+}, Cl^-, SO_4^{2-} and HCO_3^-) for all 50 samples with the Mediterranean sea water composition parameters in Fig. 10 shows a strong positive correlation coefficient for all samples from the coast and around the depression cone in the central part of the region. The correlation coefficient decreases gradually towards the south, where samples from upstream show negative correlation coefficient.

Hydrochemical facies

From the Piper diagram (Fig. 11), various hydrochemical facies were observed (NaCl, CaCl, MgCl, CaHCO$_3$, NaHCO$_3$ and CaSO$_4$). The dominant water types are CaCl and NaCl, where most of these water samples are plotted above the mixing line of sea water–freshwater. Large number of samples show NaCl type, which can indicate a strong seawater influence (Pulido-Leboeuf 2004) or upconing of deep saline water, whereas CaCl water type is an indicator of salinization and cation exchange (Walraevens and Van Camp 2005). Sources of CaSO$_4$ water type are the dissolution of evaporites intercalated within the deep sandstone layers of the aquifer and, to some extent, due to dissolution of the scattered sebkha deposits along the coast.

Hydrochemical profile and water classification according to Stuyfzand

The main chemical reaction that occurs when sea water intrudes into freshwater is cation exchange, resulting in surplus of Ca^{2+} and deficit of Na^+:
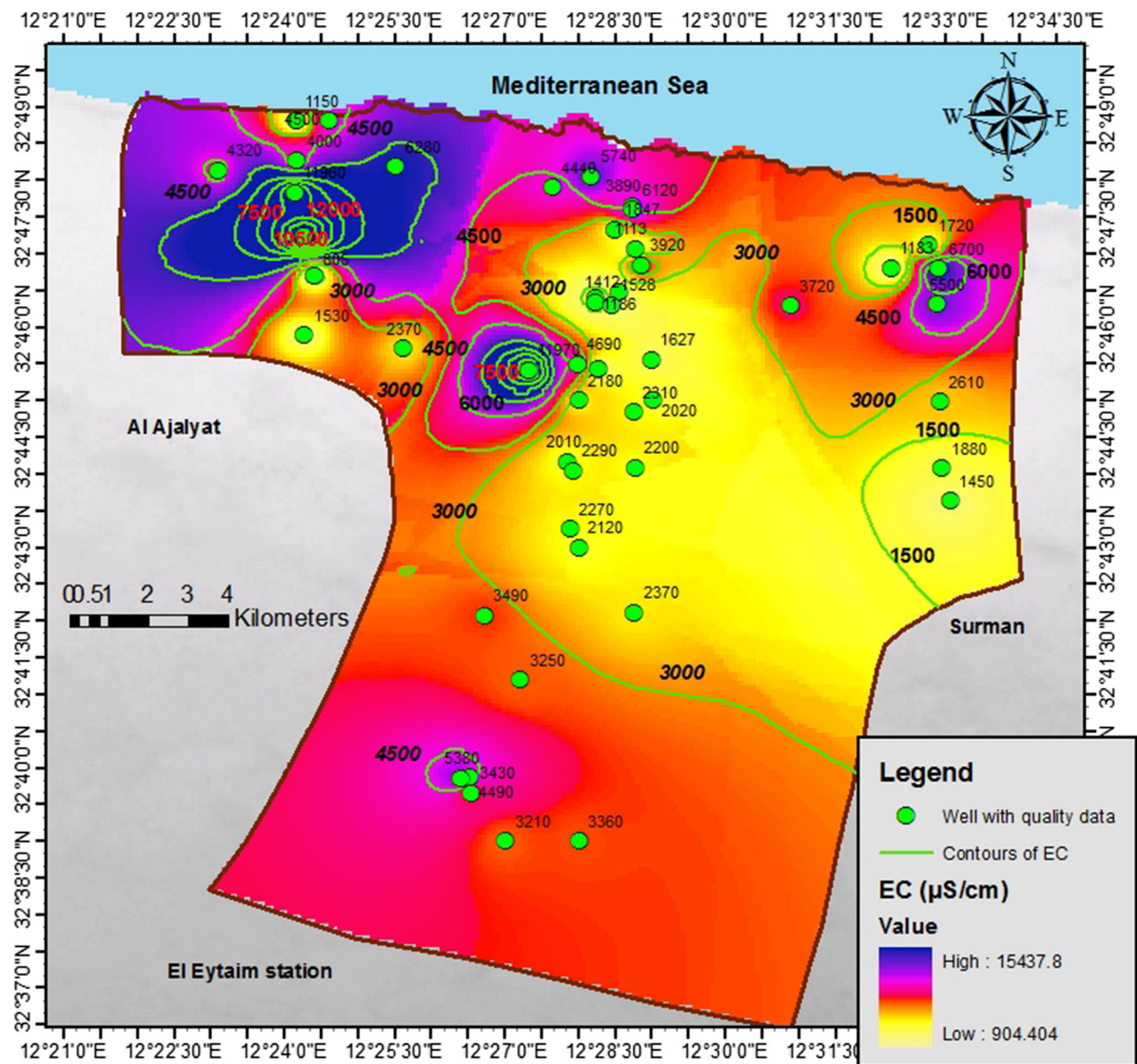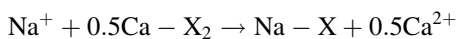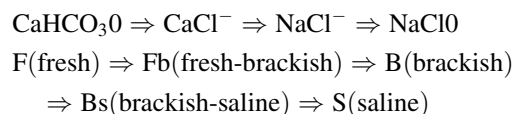
Fig. 6 Electrical conductivity map of Sabratah

$$Na^+ + 0.5Ca - X_2 \rightarrow Na - X + 0.5Ca^{2+}$$

The dominant Na^+ ions are adsorbed by the exchanger (X) and Ca^{2+} ions released, leading to the formation of CaCl water type, this is a typical water type appearing in seawater intrusion (Jones et al. 1999). The salinization evolution can be shown as follows (Walraevens and Van Camp 2005):

$$CaHCO_30 \Rightarrow CaCl^- \Rightarrow NaCl^- \Rightarrow NaCl0$$

$$F(fresh) \Rightarrow Fb(fresh\text{-}brackish) \Rightarrow B(brackish)$$
$$\Rightarrow Bs(brackish\text{-}saline) \Rightarrow S(saline)$$

Chloride can be considered a conservative tracer of water salinization, since it is not significantly affected by sorption processes or biological transformations. In addition, chloride concentrations in sea water (ca. 560 mmol/l) are significantly higher than those expected in fresh unpolluted groundwater. The chloride ion concentration thus is taken as a reference parameter (Appelo and Postma 1993). Therefore, as saltwater intrudes into coastal freshwater aquifers, the Na/Cl ratio decreases and the Ca/Cl ratio increases.

During freshening of a saline aquifer, the process is summarized as follows:
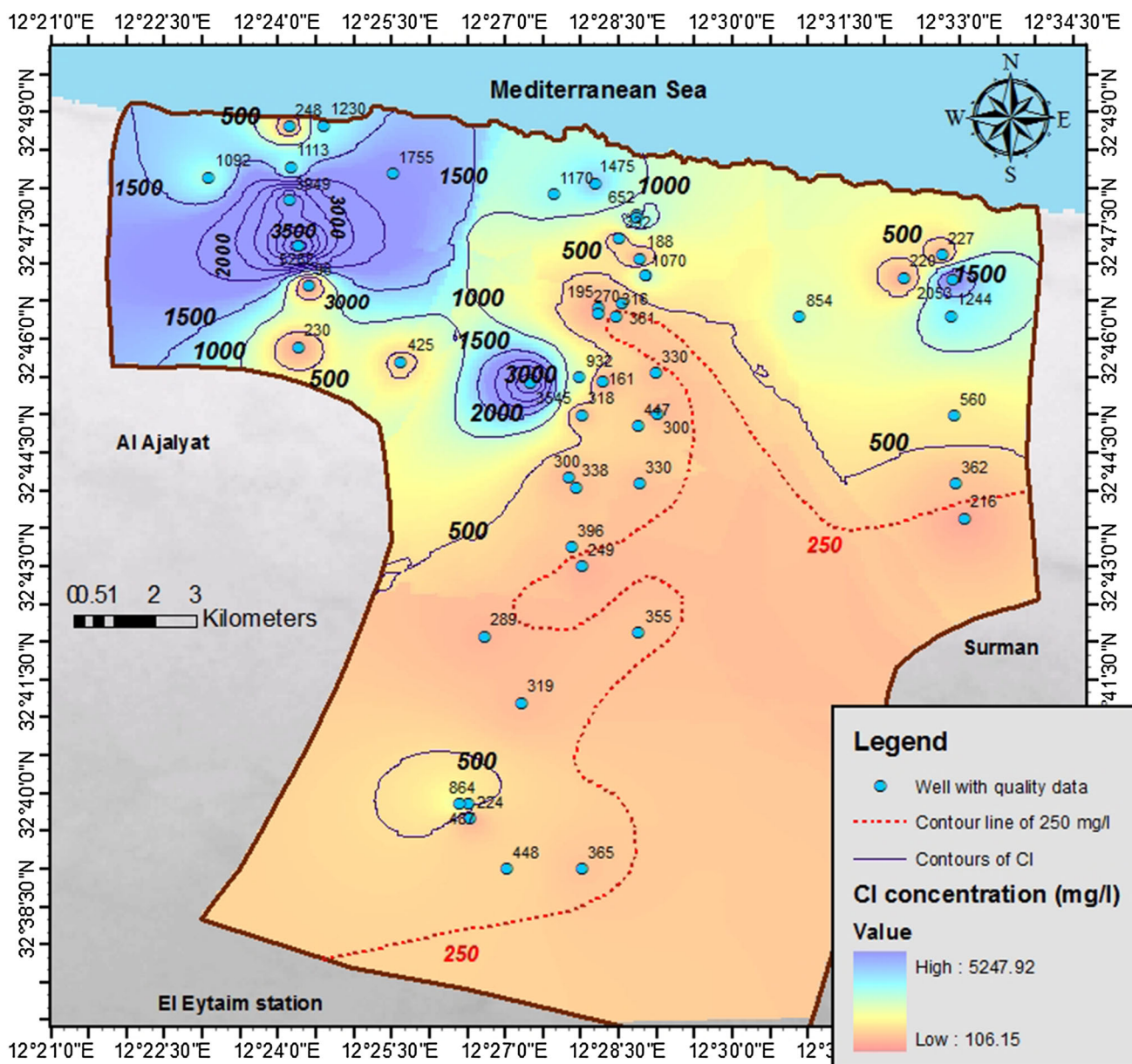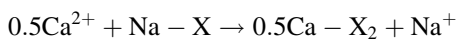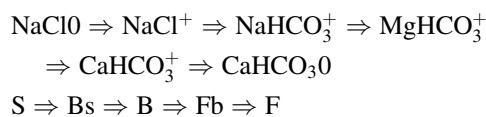
Fig. 7 Cl$^-$ map for the upper aquifer of Sabratah

$$0.5Ca^{2+} + Na - X \rightarrow 0.5Ca - X_2 + Na^+$$

Flushing of the saline aquifer by freshwater will result in uptake of Ca^{2+} by the exchanger with concomitant release of Na, where an increase in the Na/Cl ratio, and formation of the NaHCO$_3$ water type are observed, which indicate freshening. The anion HCO$_3$$^-$ is not affected because natural sediments behave as cation exchanger at the usual near-natural pH of groundwater (Appelo 1994). The freshening process can be schematized as follows (Walraevens and Van Camp 2005):

$$NaCl0 \Rightarrow NaCl^+ \Rightarrow NaHCO_3^+ \Rightarrow MgHCO_3^+$$
$$\Rightarrow CaHCO_3^+ \Rightarrow CaHCO_30$$
$$S \Rightarrow Bs \Rightarrow B \Rightarrow Fb \Rightarrow F$$

The major hydrogeochemical processes occurring in the upper aquifer are: mixing with seawater end member, cation exchange during salinization, dissolution of evaporites from the lower layer of the main aquifer or from superficial sebkha sediments, carbonate dissolution and agricultural pollution.
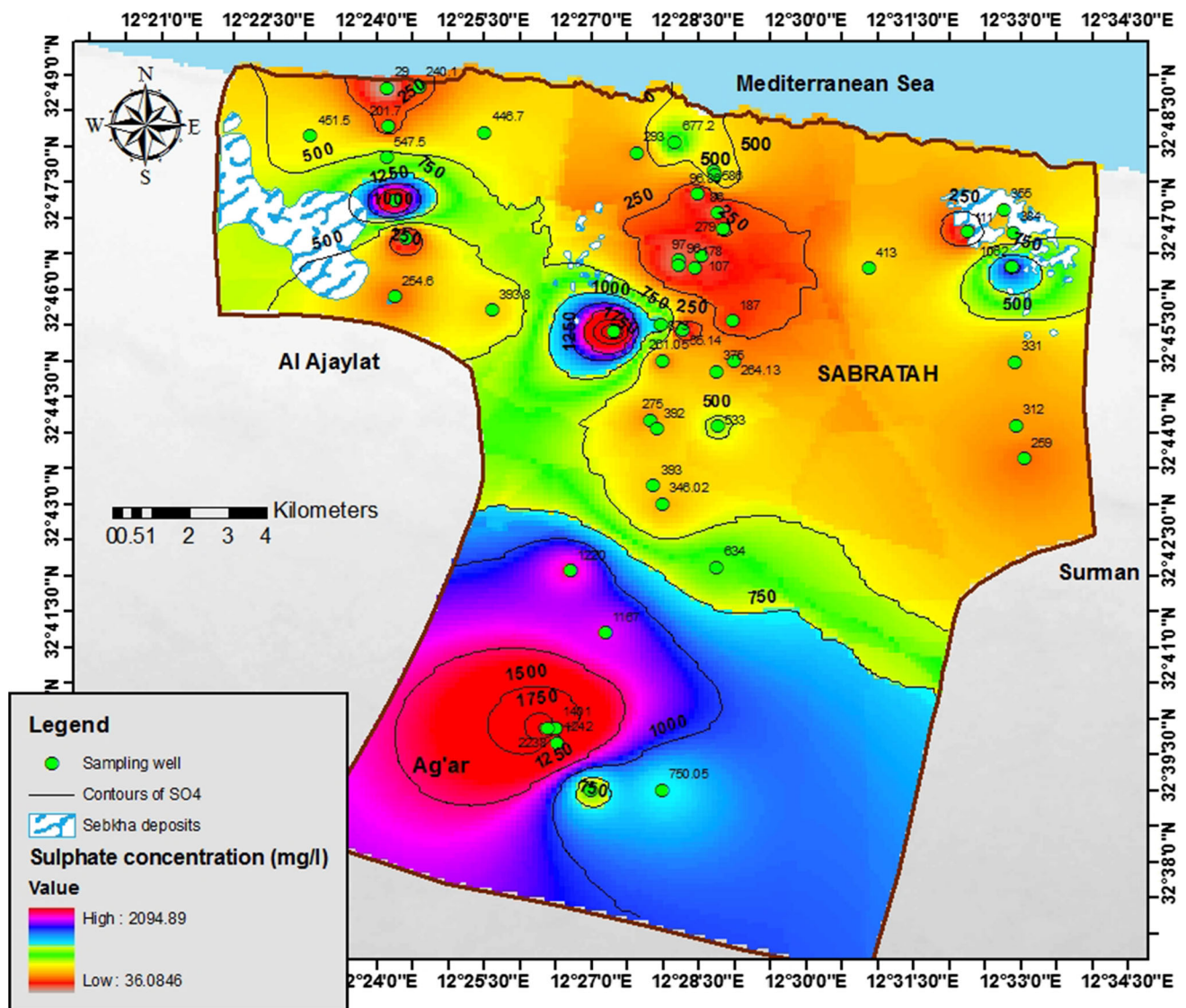
Fig. 8 SO_4^{2-} map for the upper aquifer of Sabratah

Figure 12 shows the hydrogeochemical profile in Sabratah. This is a typical example of the evolution of salinity along the flow path. The vertical position of the names of the water types has no relation with the sampling depth. The spatial distribution of water subtypes according to Stuyfzand is presented in Fig. 13 together with TDS distribution in the region.

The water classification scheme of Stuyfzand (1999) has the advantage that in brackish or saline groundwater, one can still identify many different water types even though the major anions and cations are the same and this may help to recognize processes such as upconing of more saline water in such an aquifer (Mollema et al. 2013).

Figures 12 and 13 show water type is $CaSO_4$ in the south, CaMix in the central zone and NaCl and CaCl along the coast. The NaCl type results from the strong effect of seawater intrusion. CaCl is due to cation exchange reaction

during the mixing process. At about 11 km from the shoreline (in Suq al Alalqah), $CaMix(ClHCO_3)$ evolves further inland to $CaMix(SO_4Cl)$, indicating the location of the transition zone: in this area the groundwater evolves from CaMix enriched with Cl^- ion to CaMix with SO_4^{2-} as the dominant anion. In the upstream zone, brackish extremely hard $CaSO_4$ water type is observed, up to about 20 km inland, due to the existence of the evaporitic rocks within the aquifer formation. The analytical results may additionally show a process of marine intrusion/upconing as a result of high exploitation, in the areas of the aquifer at the south of Sabratah, where the concentration of Cl^- is relatively high for many wells.

The Mg^{2+} concentration observed in several wells is mainly due to the freshwater end member derived from the recharge area, where dolomitic minerals are dissolved (Alfarrah 2011). Therefore, the positive cation exchange
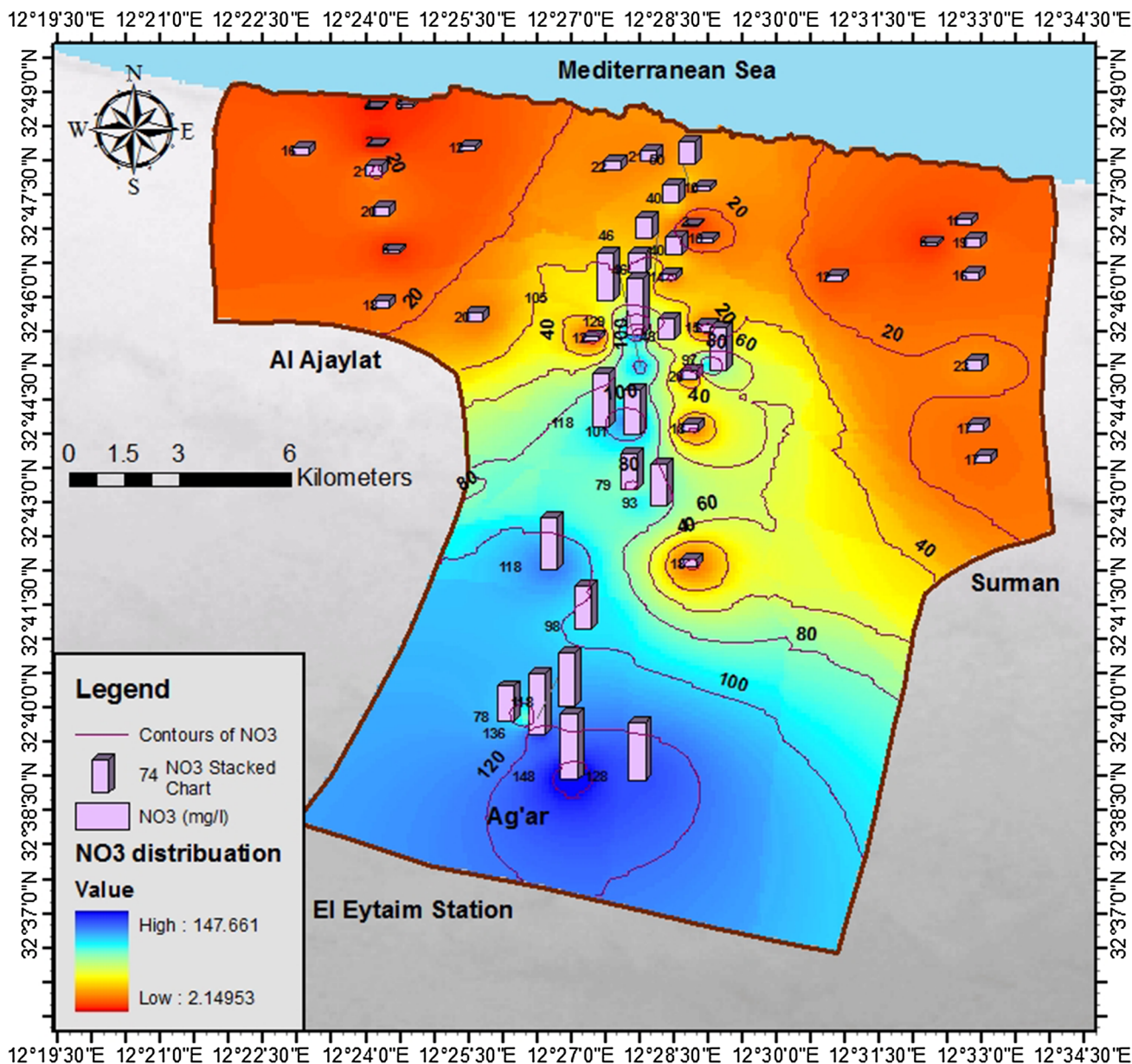
Fig. 9 NO_3^- map for the upper aquifer of Sabratah

code is in this case not pointing to freshening, as Mg^{2+} is not supplied by the marine end member (Mollema 2016). At about 11 km from the coast and downstream, cation exchange equilibrium (code "0") is found for most wells, which in this case indicates the onset of the salinization process (the value of $(Na^+ + K^+ + Mg^{2+})_{corrected}$ is decreasing as the marine cations are adsorbed during salinization).

Saturation indices

Precipitation and dissolution of calcite, dolomite, halite, gypsum and anhydrite were verified; the saturation indices

(SI) were calculated. Figure 14 shows SI values for all selected minerals.

The results show that 75% of groundwater out of 50 samples analysed is supersaturated (SI > 0) with respect to calcite ($CaCO_3$), 20% are undersaturated with respect to calcite (SI < 0) and 5% are at equilibrium (SI = 0). 60% of groundwater samples analysed seem to be oversaturated with respect to dolomite ($MgCa(CO_3)_2$) in 20% are undersaturated and 20% are at equilibrium. For gypsum ($CaSO_4·2H_2O$) and anhydrite ($CaSO_4$), 98% of samples are undersaturated. Gypsum comes close to saturation (SI > − 0.75) in many wells towards the south of the region, where the dissolution of
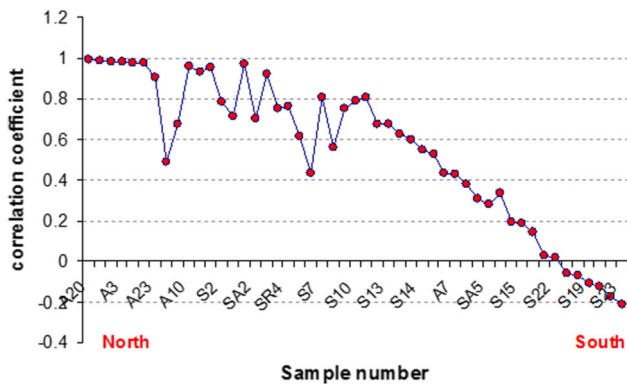
Fig. 10 Comparison of Na^+, Ca^{2+}, Mg^{2+}, Cl^-, SO_4^{2-} and HCO_3^- for all 50 samples with the Mediterranean sea water composition

evaporites from the deep aquifer layer raises the SI and for several wells near the superficial sebkha deposits.

There is a slight supersaturation with respect to calcite (SI mostly 0–1) and dolomite (SI mostly 0–2), which is rather indicating groundwater in equilibrium with those minerals. During sampling, dissolved CO_2 gas may escape, which is slightly raising pH and thus shifting carbonate equilibrium (more CO_3^{2-}), leading to SI > 0, while in situ water in the aquifer has SI with respect to calcite close to zero. So, the water in the aquifer is not oversaturated.

Fig. 11 Piper diagram for analysed samples
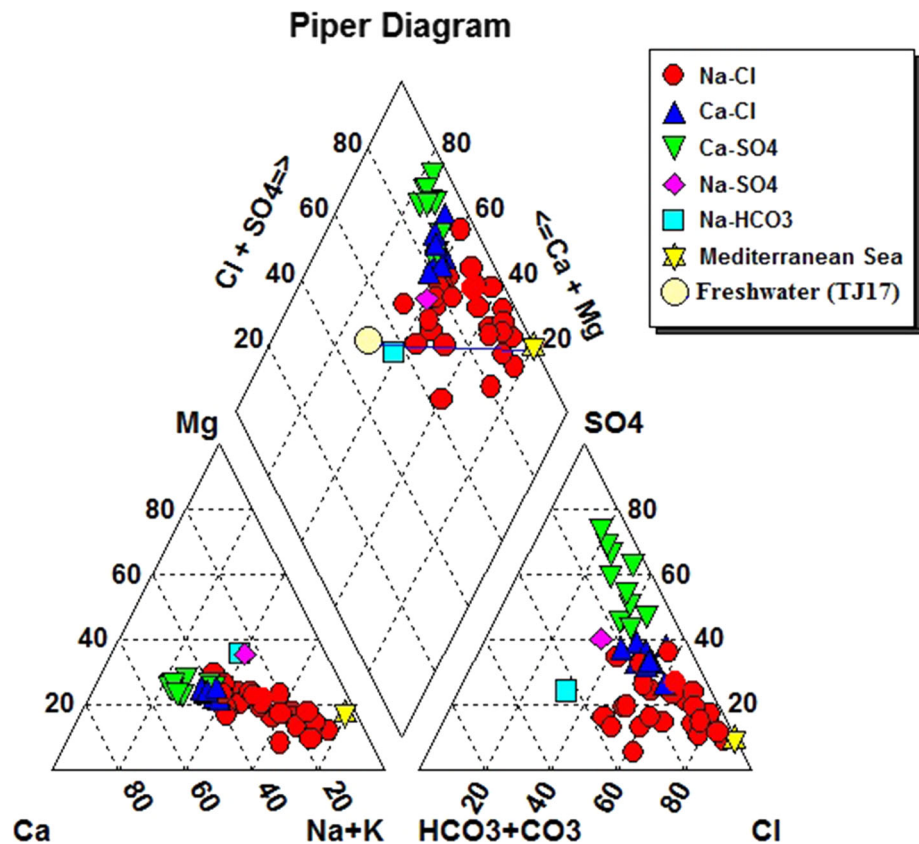
Deviation from conservative mixture of end member fraction

To confirm the importance of cation exchange processes, the difference in concentration Δn between the observed values and those expected whether mixing with sea water was the only process was calculated. Figure 15 shows the ionic deltas calculated for Na^+, Ca^{2+}, Mg^{2+}, K^+, HCO_3^- and SO_4^{2-} for all analysed samples. It is clear that the process of cation exchange due to salinization is very evident. In Fig. 15 $m_{Na+,reaction}$ (ΔNa^+) is plotted in the secondary axis; for freshwater, the ΔNa^+ is usually positive, but in this case, a large number of samples have negative values particularly in the highly saline water, down to − 23 mmol/l. The deficit of Na^+ is due to a reverse cation exchange reaction during the salinization process, where Ca^{2+} is released to the solution, while Na^+ is captured, resulting in a deficit of Na^+ in groundwater. The reverse relationship between the two ions (Na^+ and Ca^{2+}) is noticed particularly in the highly saline groundwater, where samples with large negative values of ΔNa^+ generally show strong positive ΔCa^{2+}. Potassium also shows negative (or very low positive) deltas characteristic for marine cations as a result of salinization by the intrusion/upconing of saline water.
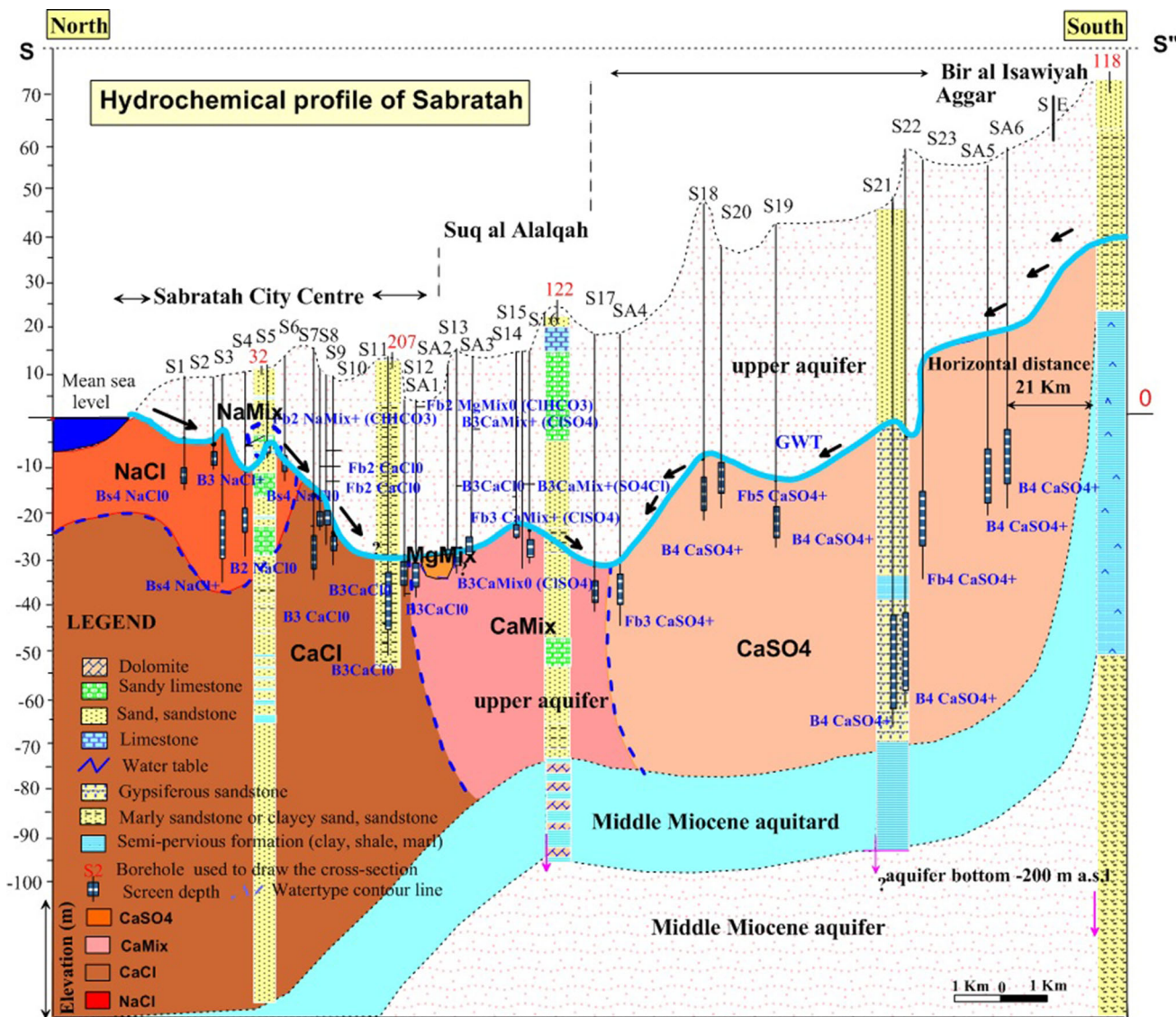
Fig. 12 Hydrochemical profile in Sabratah (location of cross section is indicated in Fig. 2)

Due to dissolution of Mg^{2+}-rich carbonate, ΔMg^{2+} is positive for most of samples. Only very few samples show a deficit of Mg^{2+}. Figure 15 also shows that the ionic delta of ΔHCO_3^- is positive for most water samples. This is due to the dissolution of carbonate minerals in the aquifer sediments. The gypsum dissolution increases ΔSO_4^{2-} to high positive values up to 22 mmol/l, where most samples show positive ΔSO_4^{2-}.

Dissolved ion relations

Figure 16 shows the scatter matrix plot for the major ions (Ca^{2+}, Mg^{2+}, Na^+, Cl^-, HCO_3^- and SO_4^{2-}). This plot shows correlations for each combination of two variables. In each row, the histogram of the entire distribution is shown, along with correlations with each of the other

variables. For example, grids 1b and 2a plot the same data (Ca^{2+} vs. Mg^{2+}), but in 1b Ca^{2+} is plotted on the y-axis, whereas in 2a, it is plotted on the x-axis.

From Fig. 16, Ca^{2+} and Mg^{2+} correlate positively and significantly with SO_4^{2-} ($r^2 = 0.78$ for Ca^{2+} and $r^2 = 0.65$ for Mg^{2+}). The high correlation coefficient $r^2 = 0.78$ between Ca^{2+} and SO_4^{2-} is pointing to the dissolution of gypsum/anhydrite from the deep aquifer layer and from the sebkha deposits near the surface. Next to the dissolution, of carbonate, a significant Mg^{2+} contribution is added from the intrusion of sea water. This can be seen by the high correlation coefficient between Mg^{2+} and Cl^- ($r^2 = 0.71$), and also between Mg^{2+} and SO_4^{2-} ($r^2 = 0.65$). High positive correlation is found between Ca^{2+} and Mg^{2+} ($r^2 = 0.85$). The concentration of Ca^{2+} in sea water is much lower than Mg^{2+}, and most of Ca^{2+} is
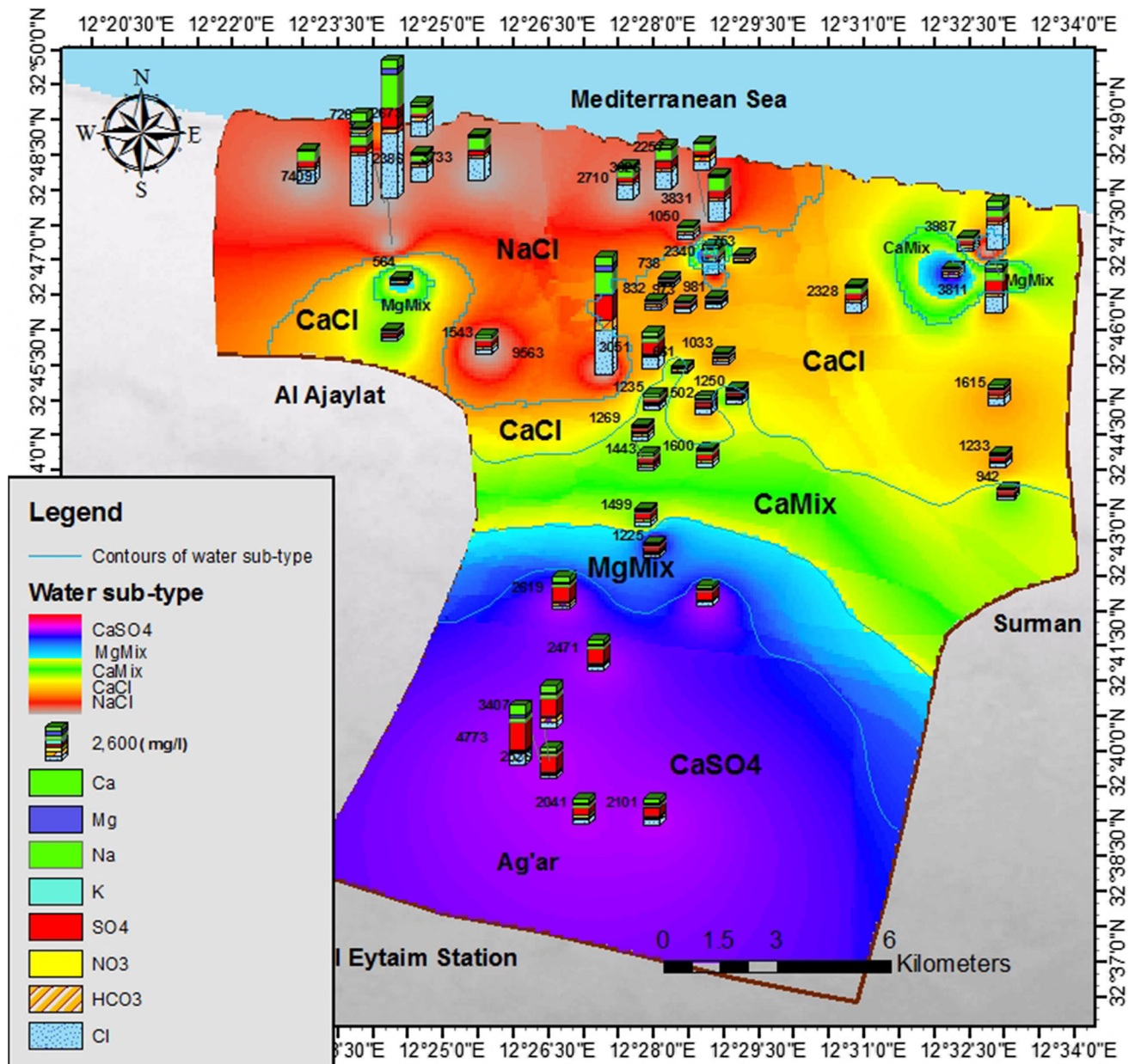
Fig. 13 Distribution of water types according to Stuyfzand with TDS concentration in Sabratah

derived from the dissolution of calcite in the freshwater aquifer and from cation exchange during the salinization process. The high correlation coefficient for the scatter plot with the linear regression line of Na^+ versus Mg^{2+} ($r^2 = 0.66$) is explained by marine intrusion. Also as a result of strong seawater influence, lower concentration of Ca^{2+} compared to Na^+ is observed close to the seaside and at the depression cones.

In the Cl^- versus SO_4^{2-} scatter plot, the low correlation ($r^2 = 0.30$) is ascribed to the additional source of SO_4^{2-} coming from the dissolution of gypsum from the deep layer of the aquifer at the south of the region.

Figure 17a, b shows the ion ratio diagrams of Na^+/Cl^- versus Cl^- and SO_4^{2-}/Cl^- versus TDS. The Na^+/Cl^- ratio in the study area ranges from 0.47 to 1.43. Lower ratios of Na^+/Cl^- (meq l^{-1}/meq l^{-1}) close to the Mediterranean seawater ratio (0.36, Fig. 17a) indicate saltwater intrusion, whereby Na^+ becomes adsorbed to the clay due to cation exchange, resulting in the deficit of Na^+ and surplus of Ca^{2+}. Just few metres from the sea and in the depression cones, very low (< 0.50) ratios are recorded. Upstream, the Na^+/Cl^- ratio is gradually rising, where it reaches up to more than 1.20. The fresh recharge water (TJ17) has Na^+/Cl^- ratio of 1.22.

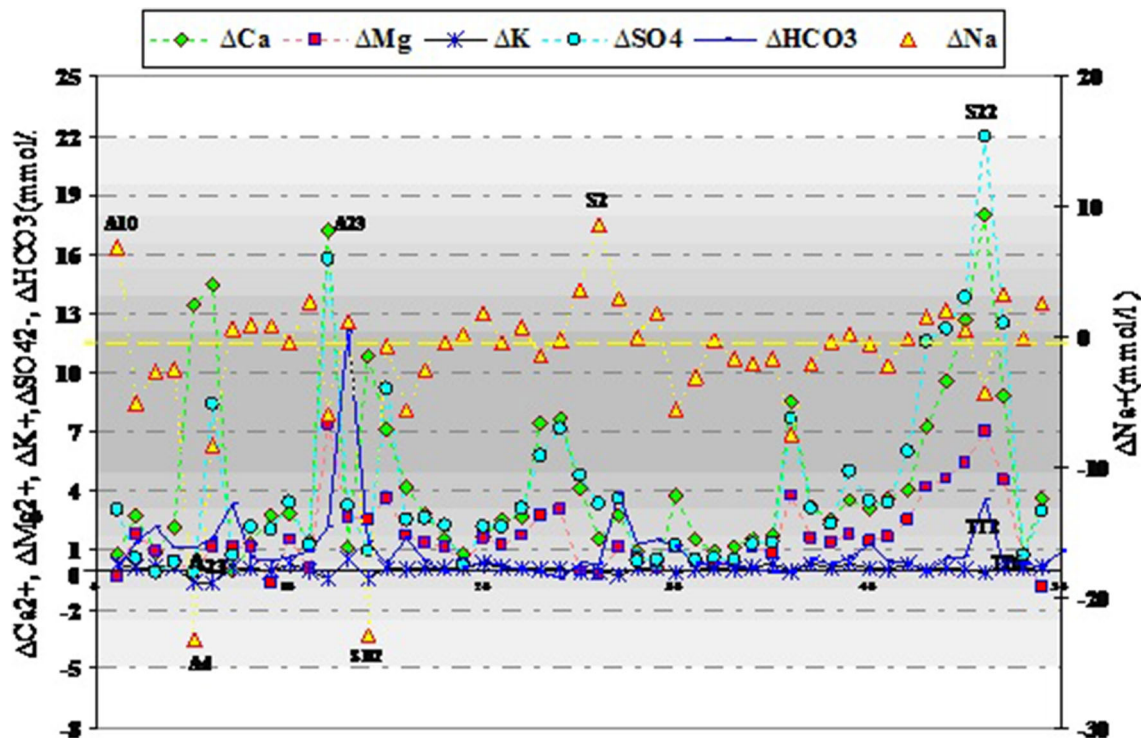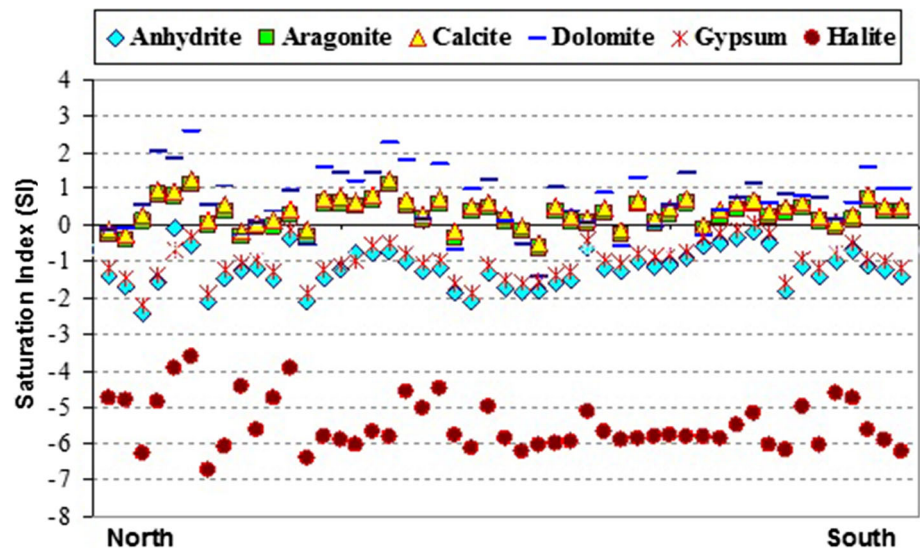Fig. 14 Calculated saturation indices of groundwater samples with respect to selected minerals

Fig. 15 Diagram of ionic delta for all analysed samples

In order to evaluate the effect of seawater mixing qualitatively, the ionic ratio SO_4^{2-}/Cl^- (mg l^{-1}/mg l^{-1}) has been plotted versus TDS (Fig. 17b). There is a wide range of scatter for the SO_4^{2-}/Cl^- ratio versus TDS, confirming that the Sabratah groundwater is controlled by other processes in addition to mixing with sea water, where samples from the south and the ones collected nearby sebkhas have a higher SO_4^{2-}/Cl^- ratio than the fresh recharge water ratio (0.66; TJ17). The other analysed samples are plotted between the ratio of 0.139 and 0.66, indicating mixing of freshwater with the Mediterranean seawater end member having ratio of 0.139.
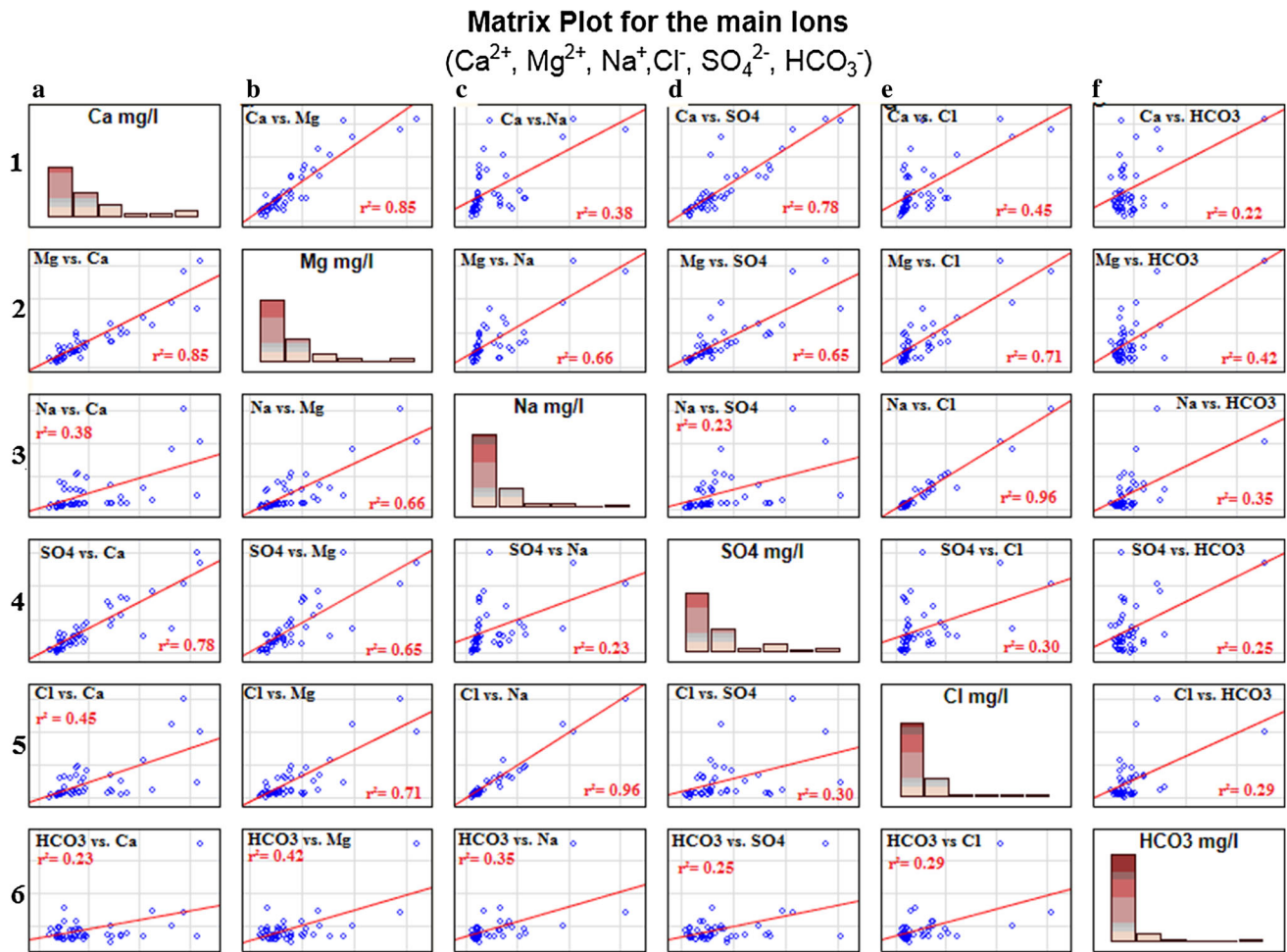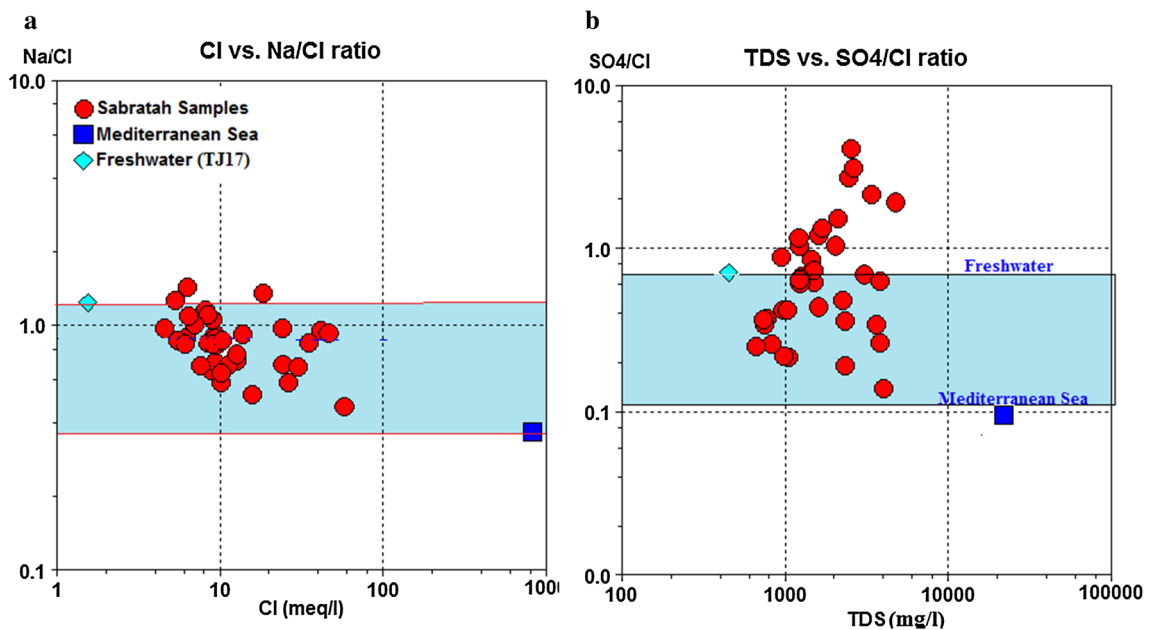
Fig. 16 Scatter matrix plot of the main ions Ca^{2+}, Mg^{2+}, Na^+, Cl^- and SO_4^{2+}

Fig. 17 a Molar ratio of Na^+/Cl^- versus Cl^- concentrations. b Molar ratio of SO_4^{2-}/Cl^- versus TDS concentrations

Conclusions

Hydrochemistry of the Sabratah shallow aquifer is very complex. The overexploitation for groundwater results in the degradation of the water quality by sea water and upconing of the deep brines. Cl^-, SO_4^{2-} and NO_3^- are the major pollutants of the aquifer.

Seawater intrusion is accompanied by chemical reactions, which modify the hydrochemistry of the coastal aquifer. The most remarkable reaction is that of the inverse cation exchange, characteristic of the changes of the theoretical mixture of sea water–freshwater, which is carried out between clays and the aquifer water. This exchange consists in the release of Ca^{2+} and the adsorption of Na^+.

Most of the observed high concentration of sulphate in Sabratah coast is coming from the effect of seawater intrusion. Additional important source of SO_4^{2-} is gypsum dissolution from the upper aquifer's formation in the upstream direction. The scattered sebkha deposits in the downstream direction, containing large amounts of gypsum, also produce high SO_4^{2-} waters.

Another most serious problem in the study area is the increased level of nitrate concentrations. It has been found that in 40% of samples, nitrate contents range between 45 and 160 mg/l. The increased content originates from leaching of nitrates from the applied nitrogen fertilizers and from sewage. It is recommended that risk assessment of nitrate pollution is useful for a better management of groundwater resources, aiming at preventing soil salinization and minimizing nitrate pollution in groundwater.

The dissolution of carbonate is another important hydrochemical process in the main aquifer. The saturation index shows mostly a slight tendency to precipitation of calcite and dolomite in the aquifer system, but this can be ascribed to lowering of CO_2 pressure at sampling, while in the aquifer, there is equilibrium with respect to these minerals.

Results show that water samples do not compare favourably with WHO standards (2008); many samples exceed the maximum admissible concentrations, highlighting the degradation of groundwater quality.

Since seawater intrusion is a severe problem in coastal aquifers of Libya, the adequate assessment of its importance is of capital interest for water resources management. Relatively simple measures such as electrical conductivity monitoring in pumping wells can serve as a proxy of seawater intrusion. Nevertheless, given the difficulty of planning and law enforcement in groundwater policies, extreme actions must be taken by the water authorities in coastal areas to find a suitable solution to this environmental crisis.

References

Alfarrah N (2011) Hydrogeological and hydrogeochemical investigation of the coastal area of Jifarah Plain, NW Libya. PhD thesis, Laboratory of Applied Geology and Hydrogeology, Ghent University, Belgium

Alfarrah N, Martens K, Walraevens K (2011) Hydrochemistry of the Upper Miocene–Pliocene–Quaternary aquifer complex of Jifarah plain, NW-Libya. Geol Belg 14(3–4):159–174

Alfarrah N, Van Camp M, Walraevens K (2013) Deducing transmissivity from specific capacity in the heterogeneous upper aquifer system of Jifarah Plain, NW-Libya. J Afr Earth Sc 85:12–21

Andersen MS, Nyvang V, Jakobsen R, Postma D (2005) Geochemical processes and solute transport at the seawater/freshwater interface of a sandy aquifer. Geochim Cosmochim Acta 69(16):3979–3994

APHA (American Public Health Association) (1985) In: Greenberg AE, Trussell RR, Clesceri LS (eds) Standard methods for the examination of water and wastewater. APHA, Washington, DC

Appelo CAJ (1994) Cation and proton exchange, pH variations, and carbonate reactions in a freshening aquifer. Water Resour Res 30:2793–2805

Appelo CAJ, Postma D (1993) Geochemistry, groundwater and pollution. A. A. Balkema, Rotterdam

Appelo CAJ, Postma D (2005) Geochemistry, groundwater and pollution, 2nd edn. A.A. Balkema, Leiden, The Netherlands, p 649

Ben-Asher J, Beltrao J, Costa M (2000) Modelling the effect of seawater intrusion on ground water salinity in agricultural areas in Israel, Portugal, Spain and Turkey. In: International symposium on techniques to control salination for horticultural productivity, Antalya, Turkey

Camur MZ, Yazicigil H (2005) Effects of the planned Ephesus recreational canal on freshwater-seawater interface in the Selcuk sub-basin, Izmir. Environ Geol 48:229–237

Chaouni Alia A, Halimi NEL, Walraevens K, Beeuwsaert E, De Breuck W (1997) Investigation de la salinisation de la plaine de Bou-Areg (Maroc nord-oriental). In: Proceedings of reports international association of hydrological sciences. Freshwater Contamination, vol 243, pp 211–220

Coetsiers M, Walraevens K (2006) Chemical characterization of the Neogene Aquifer, Belgium. Hydrogeol J 14:1556–1568

Coetsiers M, Walraevens K (2009) A new correction model for ^{14}C ages in aquifers with complex geochemistry—application to the Neogene Aquifer, Belgium. Appl Geochem 24:768–776

Coetsiers M, Blaser P, Martens K, Walraevens K (2009) Natural background levels and threshold values for groundwater in fluvial Pleistocene and Tertiary marine aquifers in Flanders, Belgium. Environ Geol 57:1155–1168

Custodio E (2010) Coastal aquifers of Europe: an overview. Hydrogeol J 18:269–280

Custodio E, Bruggeman GA (1987) Groundwater problems in coastal areas. UNESCO-IHP, Studies and Reports in Hydrology, vol 45. París, pp 1–576

Da'as A, Walraevens K (2010) Groundwater salinity in Jericho Area, West Bank, Palestine. In: Proceedings of SWIM-21 salt water intrusion meeting, Ponta Delgada, San Miguel, Azores, Portugal, pp 28–31

Da'as A, Walraevens K (2013) Hydrogeochemical investigation of groundwater in Jericho area in the Jordan Valley, West Bank, Palestine. J Afr Earth Sc 82:15–32

De Montety V, Radakovitch O, Vallet-Coulomb C, Blavoux B, Hermitte D, Valles V (2008) Origin of groundwater salinity and hydrochemical processes in a confined coastal aquifer: case of the Rhône delta (Southern France). Appl Geochem 23:2337–2349

Demirel Z (2004) The history and evaluation of saltwater intrusion into a coastal aquifer in Mersin, Turkey. J Environ Manag 70(3):275–282

Edmunds WM, Milne CJ (eds) (2001) Palaeowaters in coastal Europe: evolution of groundwater since the late Pleistocene. Geological Society of London, Special publication

GiméNez E, Morell I (1997) Hydrogeochemical analysis of salinization processes in the coastal aquifer of Oropesa (Castellon, Spain). Environ Geol 29:118–131

Gordu F, Yurtal R, Motz LH (2001) Optimization of groundwater use in the Goksu delta at Silifke. In: First international conference on saltwater intrusion and coastal aquifers monitoring, modeling, and management (SWICA-M3), Essaouira, Morocco, Turkey, pp 1–10

Grimaldi S, Angeluccetti I, Coviello V, Vezza P (2015) Cost-effectiveness of soil and water conservation measures on the catchment sediment budget—the Laaba watershed case study, Burkina Faso. Land Degrad Dev 26(7):737–747

Jones BF, Vengosh A, Rosenthal E, Yechieli Y (1999) Geochemical investigation of groundwater quality. In: Seawater intrusion in coastal aquifers-concepts, methods and practices. Kluwer, The Netherlands, pp 51–71

Karahanoglu N, Doyuran V (2003) Finite element simulation of seawater intrusion into a quarry-site coastal aquifer, Kocaeli-Darica, Turkey. Environ Geol 44(4):456–466

Kassa Teka B, Van Rompaey A, Poesen J, Van Bruyssel S, Deckers J, Amare Kassa (2015) Spatial analysis of land cover changes in Eastern Tigray (Ethiopia) from 1965 to 2007: are there signs of a forest transition. Land Degrad Dev 26(7):680–689

LIRC (Libyan Industrial Research Centre) (1995) Geological map of Jifarah Plain, 2nd edn. LIRC, Tajura

Lyles JR (2000) Is seawater intrusion affecting ground water on Lopez Island, Washington. USGS Numbered Series, U.S. Geological Survey. Fact sheet FS-057-00

Masciopinto C (2006) Simulation of coastal groundwater remediation: the case of Nardò fractured aquifer in Southern Italy. Environ Model Softw 21:85–97

Mjemah IC, Van Camp M, Walraevens K (2009) Groundwater exploitation and hydraulic parameter estimation for a Quaternary aquifer in Dar-es-Salaam, Tanzania. J Afr Earth Sci 55(3–4):134–146

Mjemah IC, Van Camp M, Martens K, Walraevens K (2011) Groundwater exploitation and recharge rate estimation of quaternary sand aquifer in Dar-es-Salaam area, Tanzania. Environ Earth Sci 63:559–569

Mollema PN (2016) Water and chemical budgets of gravel pit lakes: Case studies of fluvial gravel pit lakes along the Meuse River (the Netherlands) and coastal gravel pit lakes along the Adriatic Sea (Ravenna, Italy). PhD thesis, Technische Universiteit Delft

Mollema PN, Antonellini M, Dinelli E, Gabbianelli G, Greggio N, Stuyfzand PJ (2013) Hydrochemical and physical processes influencing salinization and freshening in Mediterranean low-lying coastal environments. Appl Geochem 34:207–221

Mollema PN, Antonellini M, Stuyfzand PJ, Juhasz-Holterman MHA, Van Diepenbeek PMJA (2015) Metal accumulation in an artificially recharged gravel pit lake used for drinking water supply. J Geochem Explor 150:35–51

Morell I, Gimenez E, Esteller MV (1996) Application of principal components analysis to the study of salinization on the Castellon plain, Spain. Sci Total Environ 177:161–171

Mtoni YE, Mjemah IC, Msindai K, Van Camp M, Walraevens K (2012) Saltwater intrusion in the Quaternary aquifer of the Dar es Salaam region, Tanzania. Geol Belg 15(1–2):16–25

Mtoni YE, Mjemah IC, Bakundukize C, Van Camp M, Walraevens K (2013) Saltwater intrusion and nitrate pollution in the coastal aquifer of Dar es Salaam, Tanzania. Environ Earth Sci 70(3):1091–1111

Parkhurst DL, Appelo CAJ (1999) User's guide to PHREEQC (version 2)—a computer program for speciation, batch-reaction, one-dimensional transport, and inverse geochemical calculations. U.S. Geological Survey water-resources investigations report 99-4259

Pulido-Leboeuf P (2004) Seawater intrusion and associated processes in a small coastal complex aquifer (Castell de Ferro, Spain). Appl Geochem 19:1517–1527

Radfar M, Van Camp M, Walraevens K (2013) Drought impacts on long-term hydrodynamic behavior of groundwater in the Tertiary-Quaternary aquifer system of Shahrekord Plain, Iran. Environ Earth Sci 70(2):927–942

Stuyfzand PJ (1986) A new hydrogeochemical classification of water types: principles and application to the coastal dunes aquifer system of the Netherlands. In: Proceedings 9th SWIM, Delft (The Netherlands), pp 641–656

Stuyfzand PJ (1993) Hydrochemistry and hydrology of the coastal dune area of the Western Netherlands. PhD dissertation, Free University (VU), Amsterdam 90-74741-01-0

Stuyfzand PJ (1999) Patterns in groundwater chemistry resulting from groundwater flow. Hydrogeol J 7:15–27

Sukhija BS, Varma VN, Nagabhushanam P, Reddy DV (1996) Differentiation of paleomarine and modern intruded salinities in coastal groundwaters (of Karaikal and Tanjavur, India) based on inorganic chemistry, organic biomarker fingerprints and radio-carbon dating. J Hydrol 174:173–201

Trabelsi R, Zairi M, Dhia HB (2007) Groundwater salinization of the Sfax superficial aquifer, Tunisia. Hydrogeol J 15:1341–1355

Van Camp M, Walraevens K (2009) Recovery scenarios for deep over-exploited aquifers with limited recharge: methodology and application to an aquifer in Belgium. Environ Geol 56(8):1505–1516

Van Camp M, Radfar M, Walraevens K (2010) Assessment of groundwater storage depletion by overexploitation using simple indicators in an irrigated closed aquifer basin in Iran. Agric Water Manag 97(11):1876–1886

Van Camp M, Radfar M, Martens K, Walraevens K (2012) Analysis of the groundwater resource decline in an intramountain aquifer system in Central Iran. Geol Belg 15(3):176–180

Van Camp M, Mjemah IC, Alfarrah N, Walraevens K (2013) Modeling approaches and strategies for data-scarce aquifers: example of the Dar es Salaam aquifer in Tanzania. Hydrogeol J 21:341–356

Van Camp M, Mtoni YE, Mjemah IC, Bakundukize C, Walraevens K (2014) Investigating seawater intrusion due to groundwater pumping with schematic model simulations: the example of the Dar Es Salaam coastal aquifer in Tanzania. J Afr Earth Sc 96:71–78

Walraevens K, Van Camp M (2005) Advances in understanding natural groundwater quality controls in coastal aquifers, 18 SWIM. Cartagena 2004, Spain, pp 451–460

Walraevens K, Boughriba M, De Breuck W (1993a) Groundwater quality evolution in the Black-Sluice Polder area around Assenede (Belgium). In: Custodio E, Galofre A (eds) Study and modelling of saltwater intrusion into aquifers. Centro

Internacional de Métodos Numéricos en Ingenieria, Barcelona, pp 121–142

Walraevens K, Lebbe L, Van Camp M, Angius G, Serra M, Vacca A, Massidda R, De Breuck W (1993b) Study and modelling of saltwater intrusion into aquifers. In: Proceedings 12th saltwater intrusion meeting, Barcelona, November 1992, pp 407–420

Walraevens K, Lebbe L, De Ceukelaire M, Van Houtte E, De Breuck W, Marras F (1994) Influence on groundwater quality of the Paleozoic Brabant Massif in Belgium due to overexploitation. IAHS Publ Groundw Qual Manag 220:461–470

Walraevens K, Cardenal-Escarcena J, Van Camp M (2007) Reaction transport modelling of a freshening aquifer (Tertiary Ledo-Paniselian Aquifer, Flanders Belgium). Appl Geochem 22:289–305

Walraevens K, Mjemah IC, Mtoni Y, Van Camp M (2013) Sources of salinity and urban pollution in the Quaternary sand aquifers of Dar es Salaam, Tanzania. J Afr Earth Sci 102:149–165

Walraevens K, Gebreyohannes T, Amare K, Hussein A, Berhane G, Baert R, Ronsse S, Kebede S, Van Hulle L, Deckers J, Martens K, Van Camp M (2015) Water balance components for sustainability assessment of groundwater dependent agriculture: example of the Mendae Plain (Tigray, Ethiopia). Land Degrad Dev 26(7):725–736

Wang C et al (2014) Assessment of river water quality based on theory of variable fuzzy sets and fuzzy binary comparison method. Water Resour Manag 28(12):4183–4200

Wang C, Yang Y, Zhang Y (2016) Cost-effective targeting soil and water conservation: a case study of Changting County in Southeast China. Land Degrad Dev 27(2):387–394

Werner AD, Ward JD, Morgan LK, Simmons CT, Robinson NI, Teubner MD (2012) Vulnerability indicators of sea water intrusion. Ground Water 50:48–58

WHO (2008) Guidelines for drinking-water quality (electronic resource): incorporating 1st and 2nd addenda, vol 1, recommendations, 3rd edn. WHO Library Cataloguing-in-Publication Data, p 668

Wildemeersch JCJ, Garba M, Sabiou M, Sleutel S, Cornelis W (2015) The effect of water and soil conservation (WSC) on the soil chemical, biological, and physical quality of a Plinthosol in Niger. Land Degrad Dev 26(7):773–783

Wu WY, Dandy GC, Maier HR (2013) Protocol for developing ANN models and its application to the assessment of the quality of the ANN model development process in drinking water quality modeling. Environ Modell Softw 54:108–127. doi:10.1016/j.envsoft.2013.12.016

Yazicigil H, Ekmekci M (2003) Perspectives on Turkish ground water resources. Ground Water 41(3):290–291

Zouhri L, Carlier E, Ben Kabbour B, Toto EA, Gorini C (2008) Groundwater interaction in the coastal environment: hydrochemical, electrical and seismic approaches. Bull Eng Geol Environ 67:123–128